Scientific Research Publishing

Open Journal of Geology, 2022, 12, 472-503
https://www.scirp.org/journal/ojg
ISSN Online: 2161-7589
ISSN Print: 2161-7570

The Permian-Triassic Transitional Zone: Jordan, Arabian Plate; Linked to Siberian Large Igneous Province and Neo-Tethys Breakup Degassing via Climate Forcing, Atmospheric Hazard and Metal Toxicity

Werner Schneider[1], Elias Salameh[2]

[1]Formerly Braunschweig Technical University, Braunschweig, Germany
[2]University of Jordan, Amman, Jordan
Email: salameli@ju.edu.jo

How to cite this paper: Schneider, W. and Salameh, E. (2022) The Permian-Triassic Transitional Zone: Jordan, Arabian Plate; Linked to Siberian Large Igneous Province and Neo-Tethys Breakup Degassing via Climate Forcing, Atmospheric Hazard and Metal Toxicity. *Open Journal of Geology*, **12**, 472-503.
https://doi.org/10.4236/ojg.2022.126023

Received: October 9, 2021
Accepted: June 27, 2022
Published: June 30, 2022

Abstract

End-Permian Gondwana siliciclastics (50 - 70 m) of the Um Irna F exposed along the NE Dead Sea, exhibit carbonate-free fining upward cycles (FUC) deposited during acid flash flood events under tropical climate. Several ferruginous paleosol intercalations cover periods of drying upward formation (DUP) under semiarid/arid climates. Thin grey pelite beds interbedded between paleosol and overlying FUC, are interpreted as tephra deposits sourced in Siberian LIP- and Neo-Tethys (NT)-Degassing. The Wadi Bassat en Nimra-section exhibits the P-T transitional zone where flash flood deposits meet supra-/intertidal sediments of the southward-directed transgressive NT. Decreasing flash-flooding continued through the Lower Scythian (Ma'in F.) during transgression, reworking, and resedimentation. Two euryhaline foraminifera-bearing limestone beds are discussed as indicators for the end of mass extinction (recovery phase: ca. 250.8 - 250.4 Ma) possibly correlating with the Maximum Flooding Surface MFS Tr 10 (ca. 250.5 Ma) on the Arabian Shelf (Khuff cycles B; A). Comparable data from the Germanic Basin as FUC/DUP-cycles, tephrasuspicious "Grey Beds" with high concentrations of As, Co, Pb, Zn, and Cu as well as the U-Pb Age data of the Siberian LIP meet the PTB-Zone between the MFSs Intervals P 40 (ca. 254 Ma)/Tr 10 (ca 250.5 Ma) on the Arabian Shelf. MFS (Tr 10, 20, 30) and SBs resp. on the Arabian Plate, as well as Scythian Substage boundaries correlate with ∂^{13} C-excursions recorded at Musandam, UAE. Thereby, the ratio of greenhouse gases (+climate forcing)/aerosols und tephra (-climate forcing) takes a significant influence on the ∂^{13}C-Variation.

Keywords

P-T Transition Zone, Jordan, Arabian Plate, Siliciclastics, Flash Flood Deposits, Neo-Tethys Transgression, Siberian LIP Degassing: Acid Rain, Tuffs, Metal Toxcicity, Climate Forcing, Milankovitch Croll Cycles, Germanic Basin (Correlation), Earth/Moon Interplay, Self-Regulation (Autopoiesis)

1. Introduction

Myths

… and rain came on Earth 40 days and 40 nights (1. Mose 7, 12).

… and the water remained150 days on Earth (1. Mose 7, 24).

… there get drowned all flesh, all animals creeping on Earth, the birds, the cattle and all that has moved on Earth, and all human beings (1. Mose 7, 21).

… and the water became abundant and rose so much on Earth that all high mountains were covered beneath the sky (1. Mose 7, 19).

… and all the water in the stream changed into "blood" (2. Mose 7, 20).

… and the fish in the stream died and the stream owned a strong smell (2. Mose 7, 21).

… and oh heaven, keep back your rain (Koran 11, 45).

From W. Jens [1], transl. Sch.

These citations reconfirmed by some 180 Ethnic Groups [2] [3], may throw a glimpse at innumerable hazardous "rare events" that have occurred throughout Earth's History.

Throughout the last decade, the authors have been dealing with: whether "rare events" (major impacting magmatic degassing), may affect apart mass extinction-sedimentologic/sequence-analytical patterns and the mineralogy of siliciclastic sediments as well?

One subject concerned Early Paleozoic and Lower Cretaceous quartz arenite fining upward cyclothems (FUC) on the Jordanian platform [4] [5], and another one focuses on end-Cretaceous transitional quartz arenite deposited in N Germany, northern Harz-foreland with regard to Deccan volcanism, India, Chicxulub impact, Mexico and volcanic arc origination (Lesser Antilles, Seychelles, Scotia) [6]; furthermore, at the latter locality (Uhry, Braunschweig County), the Eocene/Oligocene boundary in connection with both impact cratersPopigai, Russia and Chesapeake, USA [7].

To all subjects, the Atlas System, Version 3 of Price [8] was applied, telling that an abrupt change of both direction and speed of plates along their tracks would imply a major impact.

However, no definite major impact craters are known throughout the relevant Early Paleozoic (Middle Cambrian to Ordovician)! In the case of the Lower Cretaceous, we are faced with the Paraňa/Etendeka Plume Province and the opening of the S Atlantic [9] while the Cretaceous/Tertiary boundary (KPgB) relates to both Deccan Traps and the Chicxulub impact [10] [11].

Nevertheless, Price's concept appears to be inviting and helpful in order to build a bridge between "rare events", plate tectonics, and Sedimentary Geology/Mineralogy; yet the results obtained caused doubt on the main driving force by impacting versus indirect effects of plume degassing; in particular, since Deccan volcanism caused a significantly higher temperature pulse than the Chicxulub meteorite did [10].

Thus this paper stresses the main role of magmatic degassing causing climate change, atmospheric hazards, acid flash flooding (sturz rain), and global metal toxicity with regard to both biotic and abiotic "vulnerability" throughout the P-T transitional zone.

After Hercynian tectonics (Devonian-Carboniferous), following rifting and block faulting across the Near/Middle East led to splitting of this northern part of Gondwana, creating a passive margin of the Arabian Plata fronting the newly opened Neo-Tethys [12] [13] [14] [15]. Throughout the Upper Permian, the Jordanian Platform exhibited low relief plains where fluvial clastics prograded northward into the transgressive shallow Neo-Tethys [12] [16] [17] [18].

The paleogeographic position of the Arabian Platform was situated in the equatorial zone ~15˚ - 20˚ south of the paleo-equator ([19], **Figure 1**).

The P-T transitional zone falls in Jordan into the time span between both Maximum Flooding Surfaces (MFSs) P 40 (~Wuchiapingian: 254 Ma) and Tr 10 (Induan: ~250.5 Ma) established on the Arabian Plate [14] [15].

The biostratigraphic age of the late Permian Um Irna F., NE of the Dead Sea was determined by a low diversity assemblage of macroplants and palynomorphs [12] [16] [18] [20] [21] [22] with conodonts and euryhaline foraminifera indicating an early Induan age (early Triassic) [12] [16] [23] [24], after the P-T boundary events' recovery phase.

The Um Irna F. and its transitional zone to the Himara M. (lowermost Triassic) are well exposed along the NE margin of the Dead Sea some 50 - 70 m thick, along the road outcrops and several W/E-striking wadis cutting the Jordan Rift shoulder north of Wadi Mujib ([17], **Figure 2**).

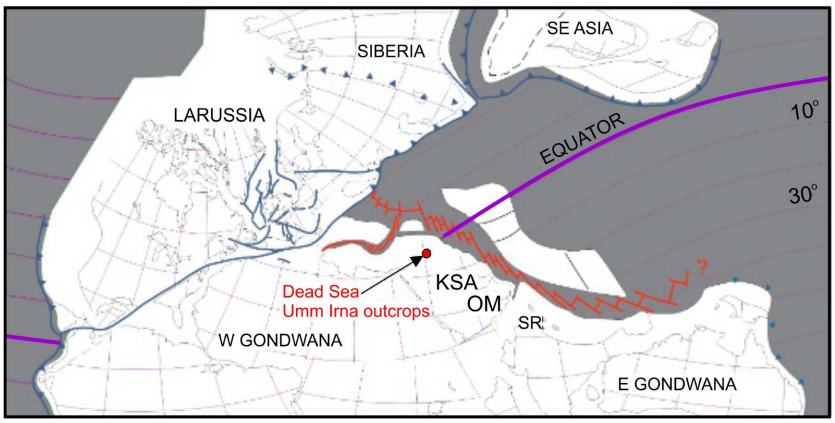

Figure 1. Paleogeographic map showing the study area (NE Dead Sea), Jordan located 15˚ - 20˚ south of the Paleo-equator (End-Permian) in the Gondwana/Neo-Tethys transitional zone under tropical climate [19].

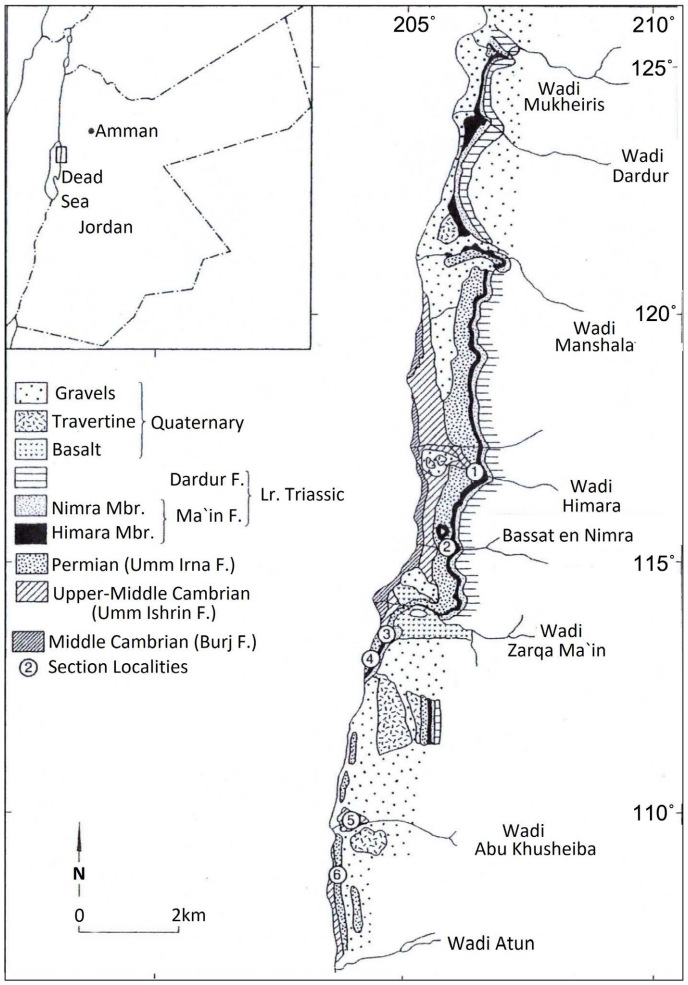

Figure 2. Locations of the upper Permian (Um Irna F./Lower Triassic Ma'in F.) wadi outcrops along the NE Dead Sea, Jordan [17].

Because of the low paleo-platform dipping the sections become seaward more complete, thicker and more fine-grained. Therefore, lithofacies correlation from wadi to wadi (Zarqa Ma'in, Bassat en Nimra, Himara) owns uncertainties [12].

Nevertheless, we are in the comfortable position to applying the biostratigraphic and sedimentologic data recovered throughout the last four decades [12] [16] [17] [18] [25] to confront them with the most recent data about the Siberian Large Igneous Province (LIP) evidence and with relating indirect effects [26].

So there does exist a general agreement on the following sedimentologic features of the P-T in Jordan transition zone [12] [16] [17] [18] [25].

- The siliciclastic fining upward cyclothems (FUC) and paleosol intercalations of the Um Irna F. were deposited on unconfined braid plains of a northwestward smoothly dipping platform of low relief close to the Tethys coastline under tropical climate by fluvial flash flood conditions.
- Each cycle originates from one single atmospheric event (sturz rain) that caused mass flow conditions to deposit complete/incomplete FUCs, nomenclature (see [27]).

- Around the Lower/Upper Member boundary of the Um Irna F., the transport direction changed from N/NW towards W/SW indicating a reorganization of nearly located source areas [17].
- The cyclic Fe-glabule/pisolite-bearing paleosols initially developedunder humid/tropical climate (hydromorphic) and then continuously changed towards semiarid/arid conditions (ascending pore water) for drying upward paleosol formation (DUP).
- Because of paleo-platform dipping and possible pre-Cretaceous down-faulting, the Upper Permian, Triassic and Jurassic sequences became thicker, more complete and faster marine, tracing northward along the Dead Sea which is most relevant for the "PTB"-interpretation (SP or hiatus-free!) [12] [16] [25].
- In contrast to other outcrops measured, the Wadi Bassat en Nimra-Section obviously exposes a hiatus-free diachronous P-T transition to the lowermost Triassic Himara M. (Fluvial → supratidal → intertidal), ([28], **Figure 3**, for comparison see [17], **Figure 4**).
- The overlying Nimra M. yields increasingly carbonate cement, ichnofacies, and two thin subtidal limestone beds bearing fully marine conodonts and euryhaline foraminifera [12] [16] [18] [23] [24] that may coincide with MFS Tr 10 (250.5 Ma) on the Arabian Shelf [14] [15].

2. Flash Flood Deposits' Architecture, Lithofacies and Mineralogic Implications

Dealing with the outcrops of both Wadis Bassat en Nimra and Himara, Miall's nomenclature ([27], **Table 1**) is applied to the carbonate-free lithofacies types of the siliciclastic cyclothems (mostly quartz arenite) while the sequence architecture relates tro liquefied/fluidized flow processes caused by flash flooding as driving transport force, hitherto applied for deep sea clastics ([29], **Figure 5**). Thereby, resedimentary processes develop from elastics via plastic to viscose-fluidal flowing mechanism between proximal and distal destination.

Atmospheric hazardous events generated, in case of the Um Irna F., five major FUCs each overlain with a kaolinitic ferruginous paleosol (0.5 - 6 m); however, all in all some 20 subordinate cycles [16] [17] [18] [28] encountered in Wadi Bassat en Nimra, as follows (**Figure 3** and **Figure 4**).

- Gmm → Sm → St → Fm → Fl → Paleosol (complete);
- Gmm → Sm → St (partially amalgamation);
- Sm → Fm → F1 → Paleosols (or missing, eroded);
- St → Fm → F1;
- Fm → F1 → Paleosols (or missing, eroded);
- Sm → Paleosols.

According to the model represented in **Figure 6** for vertical and lateral lithofacies distribution during the single flash flood, the next one may erode more or less all other preceding lithofacies units.

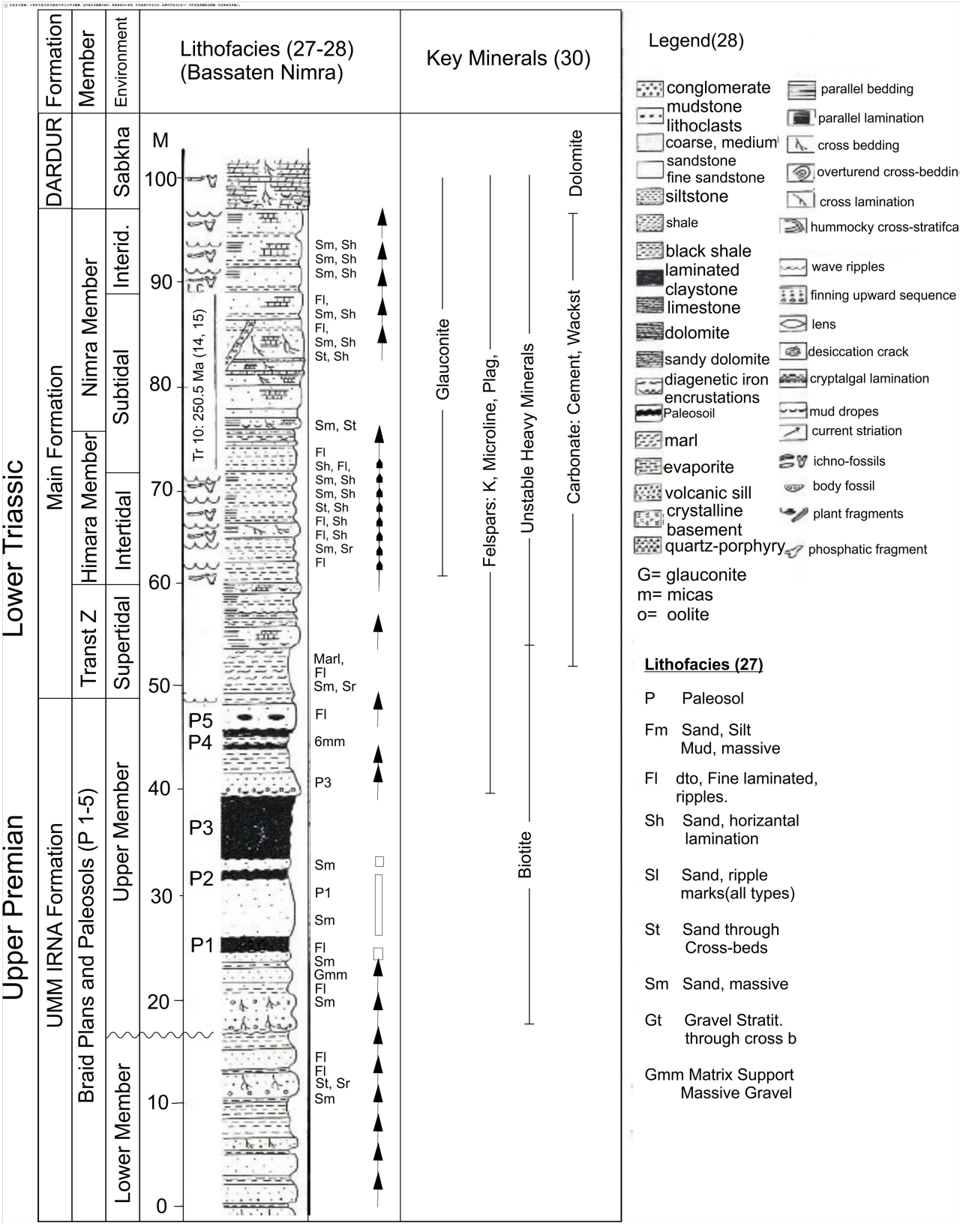

Figure 3. Lithofacies section of the Upper Permian, the transition zone and the Lower Triassic at Wadi Bassat en Nimra modified after [28]: Sedimentary environments, ichnofacies, lithofacies types [27], key mineral occurrences [30]. See fining upward cycles (FUC) and paleosol intercalations in the Um Irna F.

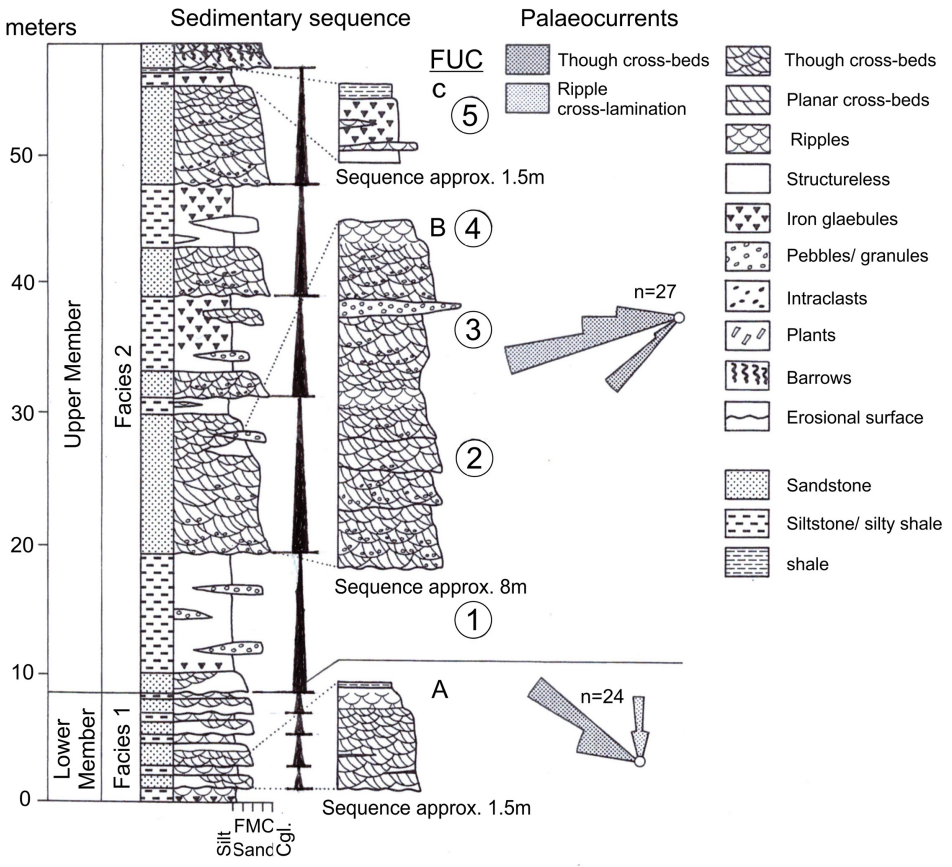

Figure 4. Lithofacies section of the Um Irna F. in Wadi Himara [17]. See fining up upward cycles FUC, paleosol beds and the change of sedimentary transport direction between the lower/upper M. of the Um Irna F.

When finally tailings of a flash flood passed into the intertidal environment during southward Tethys transgression, the silty/sandy clastics were sorted by wave and tidal current activity and thin-bedded deposited which concerns most portions of both Himara and Nimra M. **Figures 7(a)-(c)**, may illustrate such processes by using recent intertidal conditions on Amrum Island, North Sea as a model for the UmIrna F./Himara M. transional zone (paleo-aerial photograph on the braid plains of the Jordanian Platform).

Siliciclastic transport and deposition occurred in short cyclic intervals. Tectonic activity at the Lower/Upper B. of the UmIrna F. led not only to a modification of the near hinterland [17] but also to a change of mineral composition ([30], **Figure 3**). In contrast to the poorly sorted quartz arenite of the Lower M., biotite and feldspars (alkali-feldspars, plagioclase, and microcline) give evidence for an additional mica-granite source area.

Plant-bearing pelite deposited in swamps of the Upper M. provided not only palynologic age determination but also verification for paleo-wildfire [31]. Quartz grains generally angular, broken, strongly corroded, with relicts ofsyntaxial overgrowth, give hint on a manifold reworking and change of chemical//physical weathering (**Figures 8(a)-(c)**).

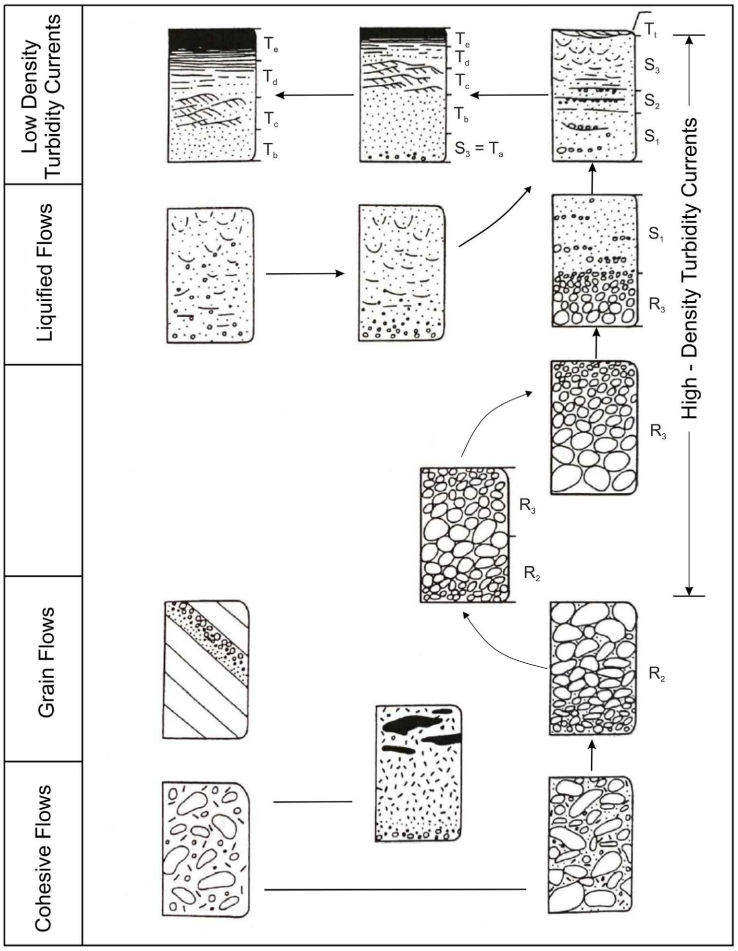

Figure 5. Stow's model of submarine flows (cohesive-grain flow-liquefied flow-low density turbidity current), [29] applied to the flash flood deposits of the End-Permian Um Irna F.

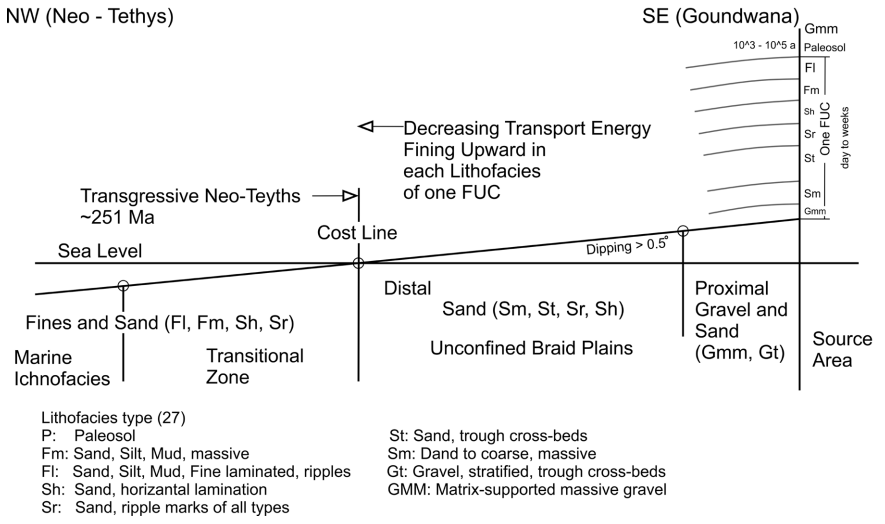

Figure 6. Model for the special distribution and sedimentation of the Um Irna flash flood deposits between source area and input into the transgressive Tethys (here: One single flash flood, FUC).

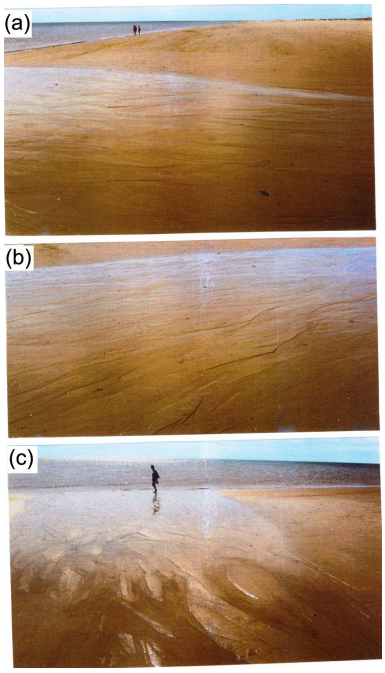

Figure 7. Intertidal environment on Amrum Island, North Sea, quasi as model for the low-dipping End–Permian platform, Jordan, (thought as aerial "photograph" of the unconfined braid plains, Jordan ((a), (b)), transgressive phase: inter/subtidal environments (c)).

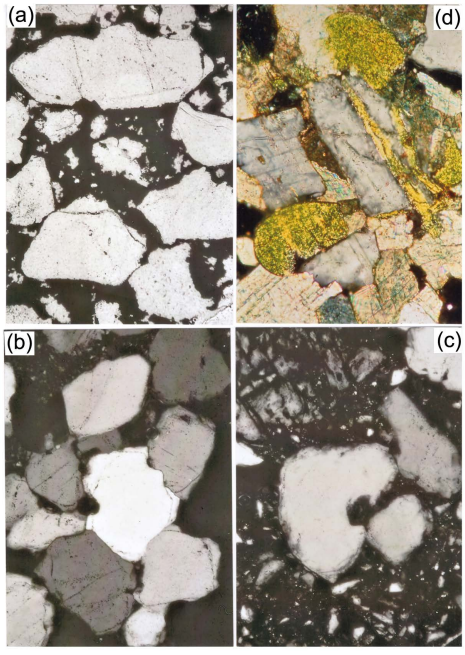

Figure 8. Thin sections of Um Irna F. and Ma'in F. sandstone. (a), (b): quartz arenite as resediment after manifold transport, resedimentation, syntaxial overgrowth, and dissolution of quartz and feldspar relicts embedded in a hematite Matrix. Seethe sharp-edged quartz fragments caused by physical weathering and paleo-wildfires ((c) [31]). (d): Arkosic sandstone (Ma'in F.) composed of quartz, feldspar and glauconite (green-yellowish) with carbonate cement. The latter works for preservation of feldspar and unstable heavy minerals.

Table 1. Light minerals, heavy minerals and cement minerals of the Um Irna F. and Ma. in F. from grain mounts and thin sections [17] [28]. Grain-%, from grain mounts and thin sections, Wadi Basset en Nimra.

Light minerals	Um Irna F.	Ma'in F.
Particles	72 - 81	72 - 83
Quartz	76 - 100	86 - 99
K-feldspar	1 - 15	1 - 10
Plagioclase	0 - 3	0 - 2
Muscovite	0 - 1	-
Biotite	0 - 4	-
Detrital matrix	7 - 12	0 - 10
Cement	8 - 16	10 - 26
Qz/F	4 -	7 - 99
Heavy minerals		
Zircon	48 - 81	14 - 61
Tourmaline	4 - 33	13 - 76
Rutile	13 - 22	3 - 25
Anatase, Brookite	2 - 4	3 - 6
Epidote (aggreg.)	0 - 1	0 - 3
Opaque	0 - 1	0 - 3
Cement minerals	Quartz syntaxial overgrowth	Quartz syntaxial overgrowth
	Kaolinite	Calcite, dolomite
	Illite/smectite mixed l.	kaolinite
	Hematite	Hematite
	Chlorite	Chlorite
	Kaol./Ill. = 2.5	Kaol./Ill. = 7.3

The ferruginous glaebule/pisolite-bearing kaolinite paleosol exposes desiccation features [12] [17] [28], (**Figure 9(c)**). The data demand short-term atmospheric hazards (days, weeks) for building up the FUCs; however, 10^3 - 10^4 a for paleosol formation. So the architectural cyclicity of FUCs was accompanied by a cyclic tropical → arid climate change (FUC → DUP).

Striking trace elements concentrations were analyzed in pelite (Ba, Co, Ni, Sr, Y, Zn, Zr, B, Sc, V) in paleosol (Ba, Co, Cu, Ni, Sr, Zr, B, Sc, V) and in Fe-glaebules (Co, Cu, Ni, Be, Zn, Sc, V, Cr, Li) (**Table 2**).

Of special interest are mm/cm-thick white-grey shaly/silty tuff-suspicious beds, always overlying the paleosols and overlain itself by the next FUC ([17], **Figure 10**), unfortunately not analyzed.

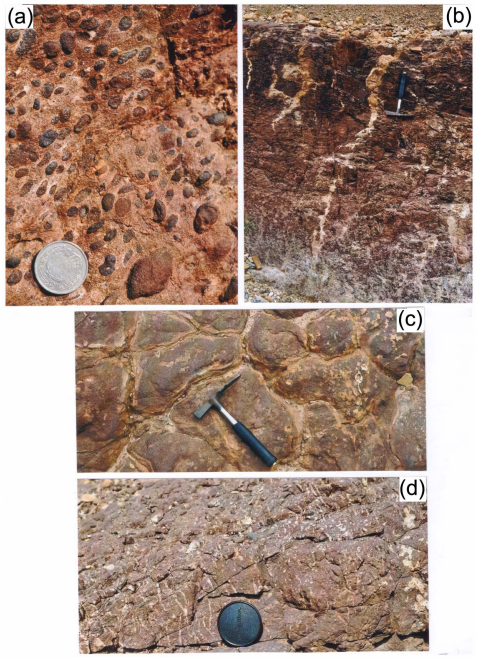

Figure 9. Pedogenetic features in the Um Irna F. [28] [30]. (a): Ferruginous glaebules embedded in kaolinite-bearing quartz arenite. (b): Sand dikes cutting pedogeneticpelite. (c): Dissication cracks in paleosol. (d): Rootlets filled with sand in pedogeneticpelite.

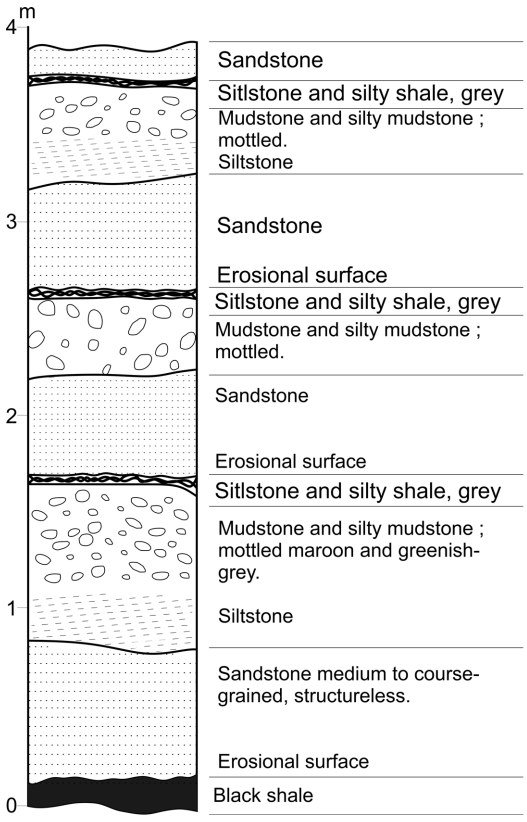

Figure 10. Grey, mm/cm thick siltstone/shale intercalations between FUCs of the Um Irna (arrows). F. Note: the tuff-suspicious thin grey beds occur always between a ferruginous paleosol and the next flash flood cycle [17].

Table 2. Major elements and trace elements of pelite and paleosol [28] and glaebules of the Um Irna F. [17].

Major elements %	Pelite [28]	Paleosol [28]	Fe-Glaebules [17]
SiO_2	50.48	50.00	18.9 - 29.0
Al_2O_3	26.72	26.07	6.1 - 11.2
CaO	0.22	0.06	0.14 - 0.18
TiO_2	1.25	0.39	0.60 - 0.89
Na_2O	0.21	0.18	0.05 - 0.07
K_2O	3.22	0.09	0.19 - 0.29
MgO	1.11	0.04	0.16 - 0.31
Fe_2O_3	7.07	14.75	54.9 - 67.8
MnO	0.01	0.01	0.01 - 0.14
P_2O_5	0.04	0.16	0.03 - 0.04
L. O. I.	12.88	-	4.40 - 7.50
Total	100	-	99.33 - 100.77
Trace elements (ppm)			
Ba	77	798	-
Co	30	18	14 - 68
Cu	3	12	5 - 16
Ni	74	30	65 - 134
Sr	60	97	-
Y	78	7	-
Be	-	-	6 - 16
Zn	74	23	41 - 131
Zr	604	230	-
B	1388	506	-
Sc	22	15	25 - 30
V	198	222	678 - 1020
Cr	-	-	109 - 300
Li	-	-	24 - 74
Rb	-	-	3 - 9

P-T Transitional Zone at Wadi Bassat En Nimra ([28] [30], Figure 3)

The upper most 20 m of the carbonate-free Um Irna F. comprise five paleosol-bearing cycles; however, in total some 15 - 20 minor hazardous FUCs of varying transport energy and completion without paleosolsunits. The last paleosol bed is overlain with the next flash flood deposit comprising reworked paleosol

pebbles (Sm → Fm).

The overlying 10 - 12 m thick more or less laminated shaly/marly red-colored clastics (subarkosic sandstone) of the Himara M. increasingly becomes calcite-indurated indicating a rising pH (>7) and the transition from continental swamp via supra- to intertidal environments during the transgressive System Tract (TST) providing diachronous lithofacies boundaries (Figure 11).

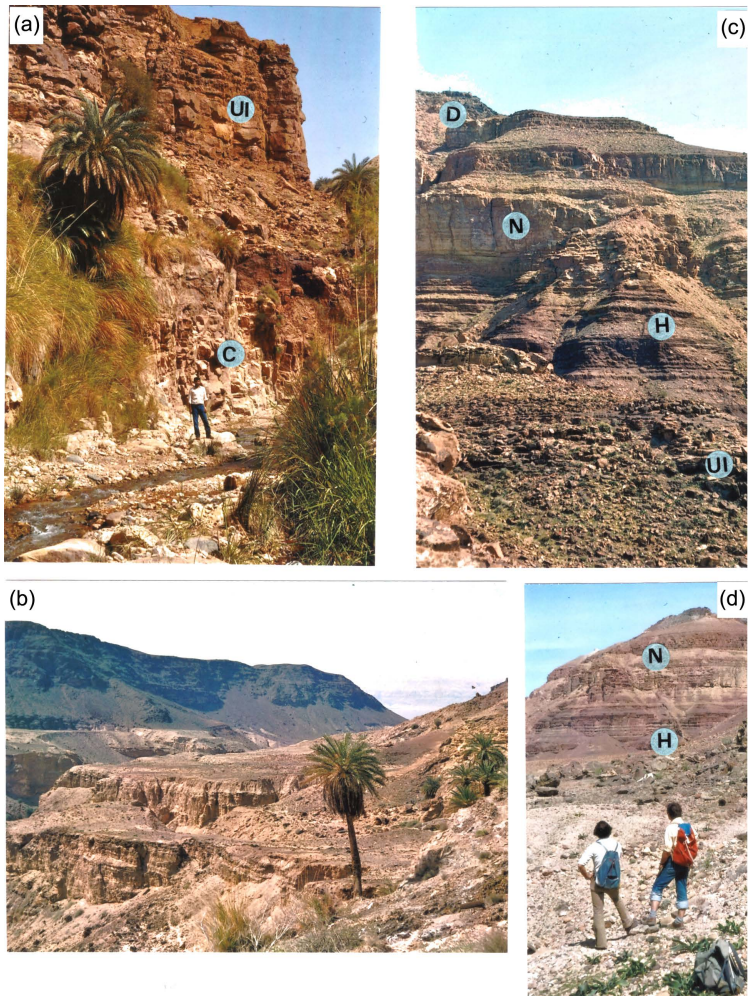

Figure 11. Field photographs from the surroundings of Wadi Zerqa Ma'in and Bassat en Nimra. (a): Wadi Abu Khusheiba II, ~2 km south of Wadi Zerqa Ma'in, with B. Amireh. Middle/Upper Cambrian quartz arenite overlain with an end-Permian paleosol and quartz arenite of the Um IrnaF. (Ul) This area is tectonically disturbed, so the overlying sequence probably belongs to the upper portion of the Um Irna F. (b): Above Wadi Zerqa Ma'in Hot Springs. Left Um Irna F., on the plateau Neolithic site (arrow). Dark Upper Triassic alkali basalt. Background: Dead Sea, West Bank, Palestine. (c): North of Wadi Zerqa Ma'in: Lower part: Um Irna F. (CUl) (H) and transitional zone to the Lower Triassic Bed sequence: Himara M. of the Ma'in F., ichnofacies-bearing intertidal. Grey sequence:Nimra M. (N) of the Ma'in F. comprising the subtidal limestone beds (wackestone) containing euryhaline fauna [12], possibly correlating with MFS Tr 10 [14] [15]. Upper part: Sabkha dolomite of the Dardur F. (d): E. Salameh and K. Bandel in front of the section above Wadi Zerqa Ma'in comprising the Himara M. (H), the Nimra M. (N) and on top the dolomite sequence of the Dardur F. (from 1978).

The following sequence (~10 m) is characterized by a burrowing ichnofacies, the first appearance of glauconite (K, Mg, (Fe^{2+}, Fe^{3+}, Al). $(SiO_3)_6 \cdot 3H_2O$), increasing carbonate cement and preserved unstable heavy minerals: hornblende, epidote, garnet [30], (**Table 1**). Glauconite represents a typical intertidal transformation from detrital biotite under defined Eh/pH conditions (**Figure 12**).

Obviously, there doesn't appear any hint on a hiatus or an abrupt change of sediment architecture across this transition zone.

The next overlying 10 m built up with grey shaly/sandy clastics, ichnofacies-free, interbedded with shell lags, culminate in two limestone beds (wackestone) 0.2 resp. 0.5 m thick. They contain conodonts and euryhaline foraminifera of early Induan age in a shallow environment of the Nimra M. ([12] [16] [23] [24], **Figure 3**, **Figure 11**).

A rich ichnofacies assemblage (Phycodes, Diplocraterion, Rusophycos, Rhizocorallium) characterizes the overlying sequenceof intertidal/supratidal dolomite (dolo-arenite) of the Dardur M. Algal lamination and pseudomorphs after sulfate neomorphism indicate coastal sabkha conditions [12] [28]. Siliciclastic intercalations mostly consolidated by carbonate cement, may be interpreted as tailing or continued continental input.

With regard to the thin tuff-suspicious beds intercalated in the Um Irna F. [31], similar deposits in the Dardur M. cause high interest for interpretation [28].

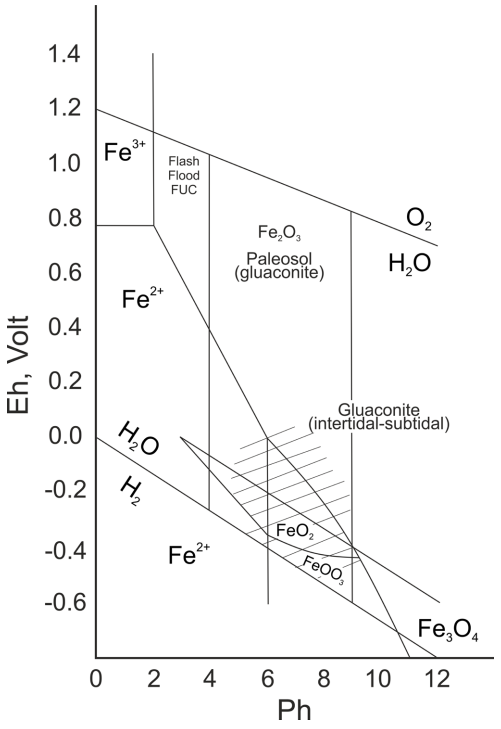

Figure 12. Eh-pH diagram showing the stability fields of common iron minerals [52]. While paleosols and flash floodsilisiclastics of the Um Irna F. indicate high Eh and low pH conditions (hematite) the subarkosic clastics of Ma'in F. (glauconite, pyrite) show typical Eh-pH patterns of a common intertidal environment.

Finally stated, the P-T transitional zone exposes a hiatus-free diachronous lithofacies transition at Wadi Bassat en Nimra throughout a tropical/arid flash flood/paleosol scenery to a shallow marine environment during a TST.

The P-T transition covers both Khuff B and Khuff A of the Saudi-Arabian Shelf, at least between the MFSs P40 (254 Ma) and Tr 30 (249.75 Ma) to be discussed below [14] [15] **Figure 13**). Comprising in connection with the Siberian LIP degassing a total time-span of 4.25 Ma, the P-T main pulse, however, concerns the interval 252.3 - 251.3 Ma [26] [32].

It has become obvious that the humid/tropical Um Irna flash flood events correlate on the Arabian Shelf (Khuff B) with a MFS; accordingly long term paleosol formation (up to several 10^4 a) coincides with a SB.

For a broader understanding of global effects by Siberian LIP degassing, additional data from Central Europe are useful [33] [34].

3. Comparison of the P-T Transitional Data with Those of the Germanic Basin/Central Europe ([32] [33] [34], Figures 14-16)

The Upper Permian Zechstein F. of Central Europe comprises seven main evaporate/siliciclastic cycles [33] [34]. Most relevant for correlation with the Jordanian Um Irna/Himara M. transitional zone is the upper most cycle (Fulda F.: z 7, **Figure 15**). The latter owns an intraformational unconformity (~251.5 Ma) and is overlain with the Calvörde F. built up with ten minor FUCs and the Bernburg F. both Lower Buntsandstein. Thereby, the commonly assigned "PTB" (~251 Ma) is to be placed ~0.2 Ma above the isochronous lithostratigraphicZechstein/Buntsandstein boundary [33] [34].

With regard to the outrunning volcanic activity, we correlate the Lower Fulda/Upper Fulda F. unconformity of the Hessian Depression ([34] [35], **Figure 15**) with the Lower/Upper M. unconformity of the Um Irna F. (**Figure 4**). In both cases re-organization of the near-located source areas and change of sediment transport direction took place.

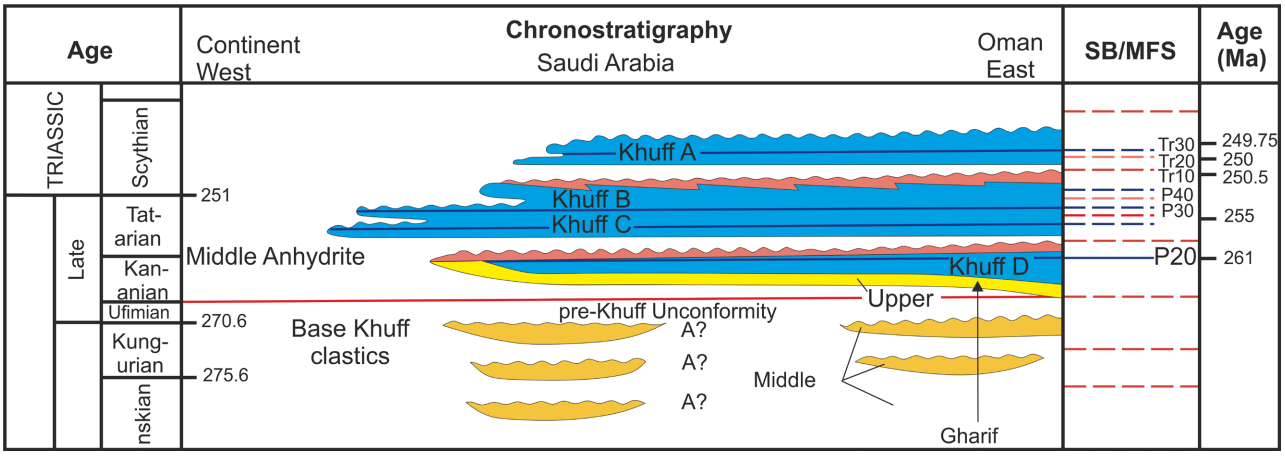

Figure 13. The P-T transitional zone (Um Irna F.,-Ma'in F.) on the Jordanian Platform relate to the Kkuff cycles B-A of the Arabian Shelf [14] [15] and is placed between both MFSs T 40 (254 Ma) and Tr 10 (250.5 Ma).

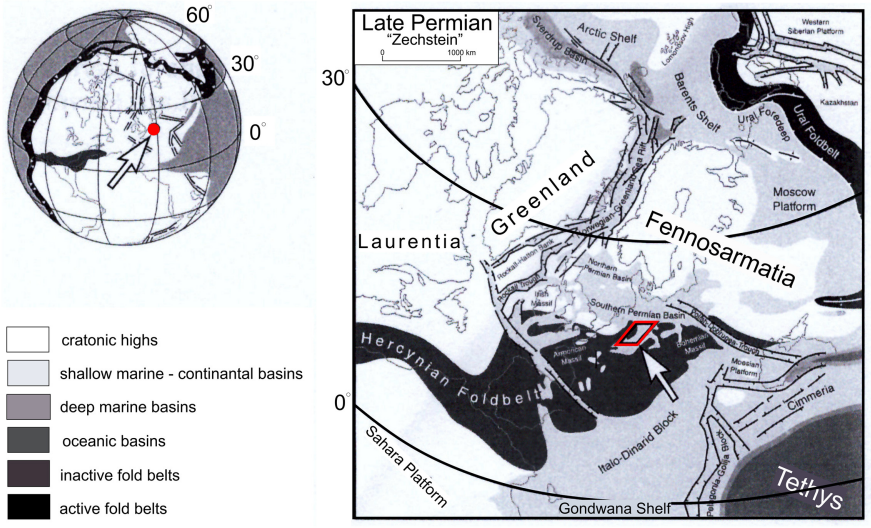

Figure 14. Paleogeographic map (Late Permian) of the Northern Hemisphere. Rhomb and spot: Germanic Basin [32].

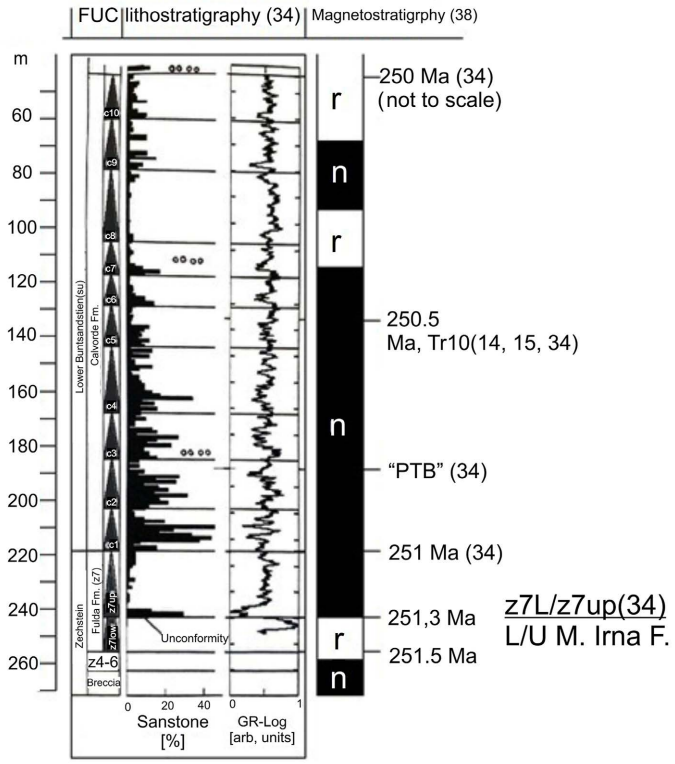

Figure 15. Lithostratigraphy of the Upper Zechstein (End-Permian)and of the Lower Buntsandstein (Scythian) in Wulften-1 drill hole, Hessian Depression, Germanic Basin [33] [34] [35]. Note the transitionzone (z7up/c1: 251.2 Ma), and the unconformity Lower/Upper Fulda F. (251.5 Ma), and the 10 minor FUCs of the Calvörde F. MFS Tr 10 may fall into c6 cycle (250.0 Ma), Tr 20 may coincide with the Calvörde/Bernburg F. boundary (250.5 Ma). The hitherto assigned "PTB" (251 Ma) would be located within c2. The 00000-beds represent calcoolite beds indicating short temperature rise. These age data are based on [35] and combined with uncertainties. Magnetostratigraphic analysis show normal magnetization for the P-T transitional zone [38].

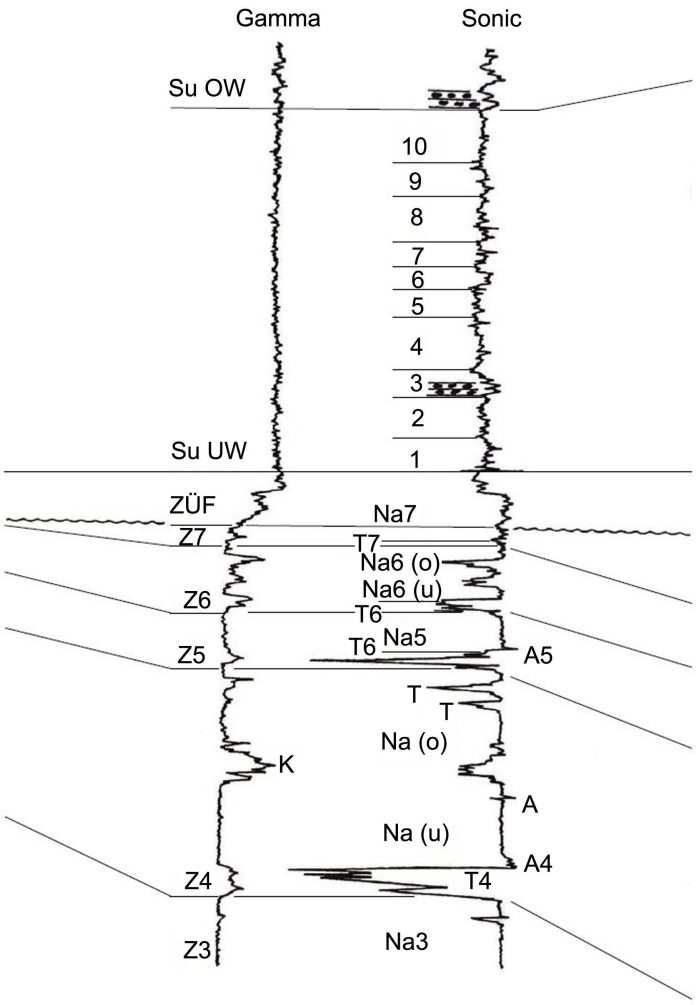

Figure 16. Sonic and gamma ray logs represent the cyclicity of evaporates (Na 3 - 7) and pelites (T 4 - 7) of the Upper Zechstein (z 4 - 7) and theCalvörde F. (su UW 1 - 107) in the Central Helgoland Basin, North Sea [36]; z 7/z ÜF: unconformity, calcoolite beds at base of c 3 and of the Bernburg F. Because of tectonic quiescency across the P-T transition zone the lithostratigraphic boundaries of the Calvörde cycles own isochronous character throughout wide parts of Central Europe. Note the symmetric volume distribution of sand in each cycle.

Around the "PTB" a general trend from evaporiticsabkha to playa facies developed in the Germanic Basin while on the Jordanian Platform hazardous atmospheric events caused cyclic flash flooding (super cyclones) under tropical climatic conditions with subsequent drying upward paleosol formation by increasing aridity (5 major cycles, 20 minor cycles). On the Arabian Shelf the Khuff Cycles B, A dominates this time-span (**Figure 13**).

Based on tectonic quiescence, the Zechstein/Buntsandsteinlithofacies boundary appears as isochronous which is well documented across the Helgoland Basin, North Sea ([36], **Figure 16**), while the Um Irna/Ma'in F. boundary at Wadi Bassat en Nimra, Jordan exposes a hiatus-free continental/marine transitional sequence during transgression, however, of diachronous character.

The Calvörde F. (10 minor FUCs: **Figure 15**: each 100 kyr) that can be reliably traced across Central Europe (Netherlands–Poland), was very probably directed by perturbation cycles of Milankovitch origin [3] [4] [37]. Thereby, a few calcoolite interrelations in the siliciclastic cycles indicate short-term playa conditions.

High resolution geochemical analysis of the siliciclastic minor cycles from the cored Wulften-1 borehole, NE Hessian Depression [34] provides significantly high concentrations of toxic metals (As, Co, Cu, Pb, Zn, *et al.*) hosted in grey colored pelite beds of the Fulda F. (z 6, z 7, z 7 low/z 7 up, z 7 top) as well as through the Calvörde F. (c 2, c 7, c 8; **Figure 17**). These thin white-grey-greenish pelite beds challenge an interpretation of tuff layers, as also encountered overlying paleosols in Wadi Himara, Jordan [17]. Are they really tuffs sourced in Siberian LIP degassing?

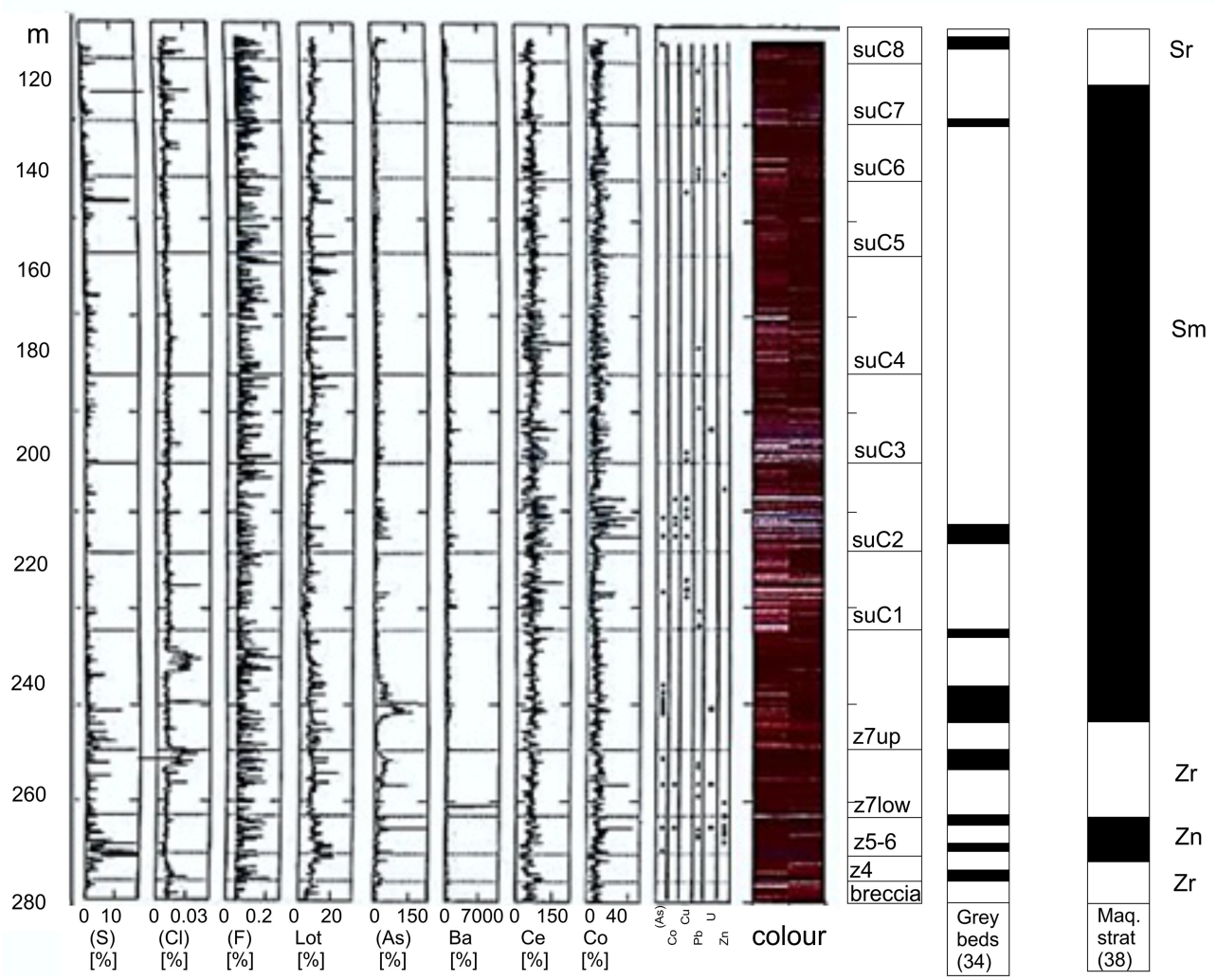

Figure 17. Lithostratigraphic color column of drill hole Wulften-1 for the section z 4 → suC8. According to [34] the socalled grey beds would represent anoxic conditions (tuff-suspicious?). The most striking grey beds assigned are geochemically characterized by higher concentrations of both As and Co resp. by Cu and Zn. **Table 3** lists the possible As, Co minerals typical for the exhalative phase during magmatism. The major sequence of the P-T transitional zone covers the time-span of normal magnetization comprising most of the grey beds.

Astronomical tuning by spectral gamma ray logs of the P-T transitional zone through marine hiatus-free sections in S China [37] and integrated magnetostratigraphic scaling of climate cycles [38] in the Germanic Basin [33] provide substage boundary ages of the Lower Triassic relative to an assigned 251.902 ± 0.024 Ma age of the PTB [39] [40] and for recurrent carbon isotope excursions through the Early Triassic.

Figure 18 shows high resolution $\partial^{13}C$ fluctuations based on conodont biostratigraphy from Early Triassic shallow marine carbonate to rocks of the Musandam Peninsula/United Arab Emirate [40] for finding approach to the Jordanian Platform, Arabian Plate, NGondwana.

Here we apply the substage boundary data of Li *et al.* [37] and the sequence analytical data (MFSs, SBs: [14] [15]) for further evaluation in connection with the Siberian LIP magmatism [26].

4. The Siberian LIP: Implications to Climate and Sedimentary Geology across the P-T Transition Zone (Jordanian Platform, Intercontinental Germanic Basin)

For tracing the influence of the Siberian LIP on the target areas in Jordan and Central Europe, the following compiled age and petrologic data are highly appreciated [26].

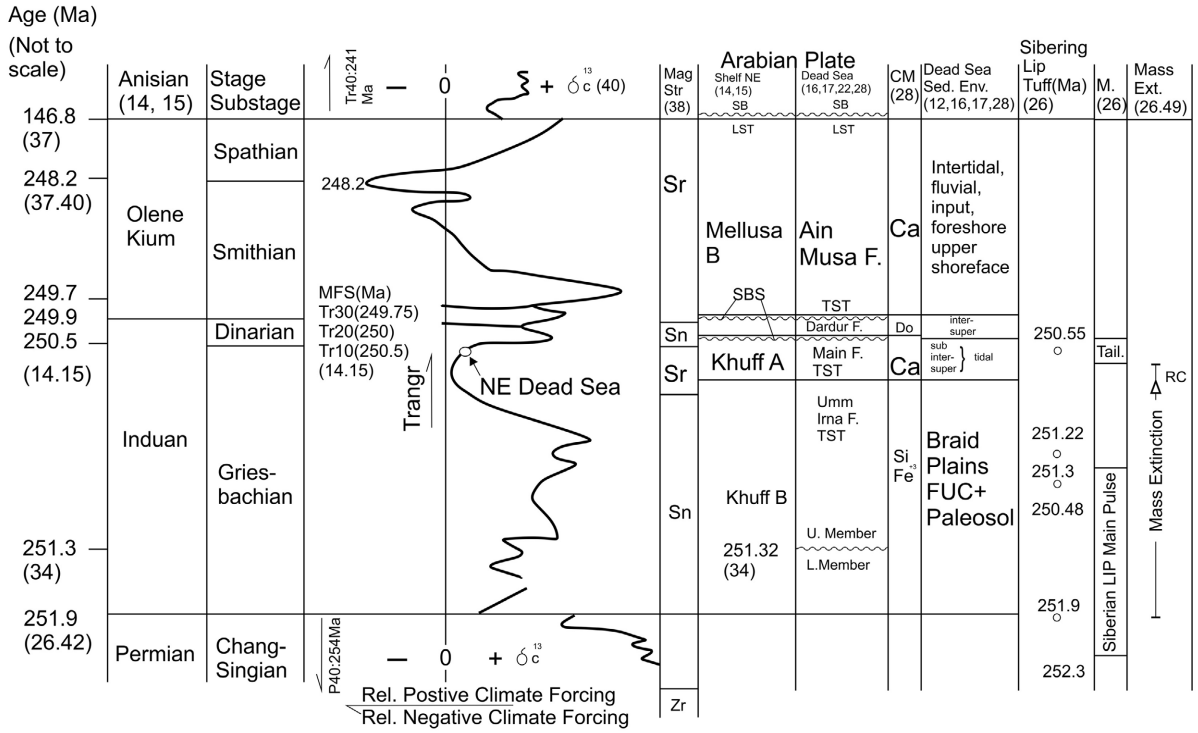

Figure 18. $\partial^{13}C$ fluctuation for the time-span 252.3 - 245 Ma analyzed by end-Permian/Lower Triassic conodont-bearing carbonate rocks of the Musandam Peninsula, United Arab Emirates for N Gondwana [40]. Ages (Ma) are not to scale. Substage dating [37], magnetostratigraphy [38], sequence analytical data (MFSs, SBs) of the Arabian Plate [14] [15] further age date [26] [39] [42] are tentatively used for correlation purposes with the $\partial^{13}C$ curve. CM cement, Mmagmatism, Mag Magnetostratigraphic, RC Recovery Phase.

- The track of Siberian for the period 260 - 240 Ma is anchored at the head of the TazovskaGuba (TG in **Figure 19**) and changes through an angle of 70˚ at 250 Ma by a six fold increase in rate of plate movement [8].
- The Tungaska basin itself hosts the main Siberian Trap Basalt sequence (Central Basalt Flow) owning a volume of ~2.5 M·km^3. However, most recent investigations document an additional spread of magmatic rock volume (~20%) across the Taimyr Belt, the Yenisei/Khatanga Trough, and the Maymecha/Kotny area, so covering in total ~5 Mm^3 recovered by outcropping, sedimentary imaged and by drilling ([26] [41], **Figure 20**).
- The main pulse of volcanic/subvolcanic activity covers the time span 252.3 - 251.3 ± 0.11 Ma based on the first high precision U-Pb zircon geochronology [39] [42]. The basalt flows of both Taimyr Peninsula and Tunguska Basin show a synchronicity of ~100.000 a error bar.
- During increasing exploration it has become obvious that the magmatic spectrum comprises–apart from tholeiitic flood basalts-a broad variety of alkaline (ultra)-mafic to felsic intrusive complexes, layered intrusive bodies, plutons, sill, and dykes [26]. So the magmatites of the Yenisei/Khataga Trench reveal syenite, granite, quartz-syenite, carbonatite, and monzo-syenite, partly displaying crustal assimilation while alkaline lavas ascended rapidly without crustal interaction. Accordingly, trace elements assemblage dissolved in magmatic gas is expected to be exceptionally high.
- In the Siberian LIP commonly tholeiites build up the lower portion of the lava pile intruded and penetrated by the scarcely younger alkaline rocks in the Maymecha/Kotny area. The latter exposes a broad petrochemical composition (12 distinct geochemical lava units in the Norilsk region). Alkaline series include trachy-dacite with evolved composition (>60% SiO_2).

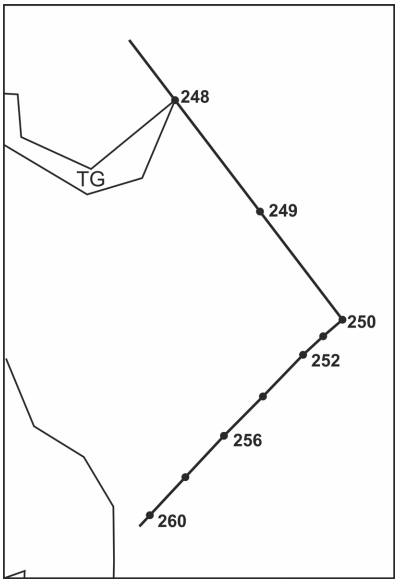

Figure 19. Track of Siberia from 260 - 240 Ma is anchored at the head of the Tazovska-Guba (TG). It shows an abrupt change at 250 Ma through an angle of 70^0 and a six fold increase in the rate of plate movement.

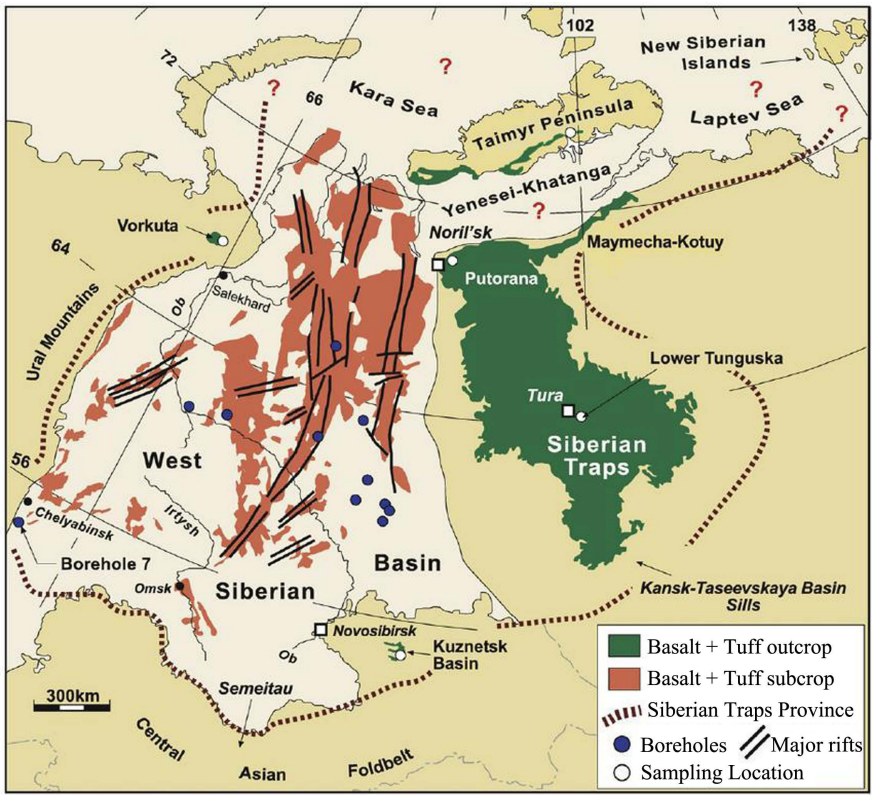

Figure 20. Overview of the Siberian LIP [41] comprising the Tunguska Basin, the Taimyr area and the Yenisei Khatanga Depression.

- A final emplacement of monzo-diorite (250.8 - 250.4 Ma) associates with the main Siberian main rock suite.
- Trachyte tuff (251.904 ± 0.061 Ma) and trachy-rhyodacite tuff (251.483 ± 0.088 Ma) are known from the Delkansky F. [39] [41]. Other ash beds yield an U-Pb zircon age of 251.22 ± 0.02 Ma) [42] resp. 250.55 ± 0.51 Ma [43] [44].
- Apart from primary magmatic gas, there are additional drivers for atmospheric implications like a) (CO_2 and CH_4 (100.000 Gt) via contact metamorphism with organic-rich and petroleum-bearing Paleozoic sedimentary rocks around sill intrusions (1.6 M·km^2) in the Tunguska Basin plus 20% of subvolcanic intrusions in both Taimyr and Yenisei/Khatanga area [45], and b) primary CH_4 sourced in the Lower Mantle [46].
- Alkaline rocks of the Taimyr Fold Belt were previously dated by ^{40}Ar-^{39}Ar, U-Pb secondary ion mass spectrometry on between 249 - 230 Ma and interpreted as tailings of the main Siberian LIP [47]. However, none of these rocks were dated by high precision U-Pb zircon geochronology; so uncertainties are large and data questionable.
- Since depending on the petrochemical magma variety, its origin and ascent through mantle and crust rocks suits, a broad spectrum of volatiles including toxic metals dissolved, are expected to have massive influence on atmosphere, hydrosphere, rock mineralogy, and biosphere [48] [49].

The most important magmatic gases are H_2O, (35 - 90 Mol-%), CO_2 (5% - 50%), SO_2 (2% - 30%), HCl and HF [50]. Gas compound in magma and time of gasemanation during ascend depend on the silicate melt composition. Accordingly, because of low viscosity basaltic melts have a fast ascent through mantle and crust while SiO_2 richer melts may differentiate and react with the rock column [26] [45].

Many elements dissolved in magmatic gas are precipitated as chloride (Na, K, NH_4, Ca, Pb, Mn, Fe), fluoride (Na, Mg) nitride (Fe), sulfate (S, Se, As, Pb, Cu, Co, Hg, Zn, Fi, Ni), oxide (Mg. Cu, Pb, B) and arsenide (Fe, Co, Ni) during cooling down and reaction with the atmosphere [51] [52] [53].

Most relevant for correlation attempts to both target areas (Jordan, Germanic Basin) are the geochemical data available from borehole Wülften-1, Hessian Depression ([33] [34], **Figure 7**) with a main focus on As, Co and Cu-minerals (AsS, As_2S_3, Cu_3AsS_4, (Cu, Fe, Zn), As_2S_3, FeAsS, CoAsS, $CoAs_{2\text{-}3}$, Co_3S_4, CuS, CuO [51] [53]. During weathering primary As, Cu-minerals react with $O_2$to arsenolite/claudetite (As_2O_3), *i.e.* $2FeAsS + 5O_2 \rightarrow Fe_2O_3 + 2SO_2 + As_2O_3$ [53].

Arsenolite represents itself as a white/grey powder that may influence the color of tuff deposits which already carried the primary As, Co-minerals to the depositional site.

Indeed the thin grey pelite beds intercalated between paleosol and the next FUC of the Um Irna F. ([17] **Figure 10**) and the color change (red-grey) at the Himara/Nimra M. boundary as well as the so-called "grey beds" intercalated through the P-T transition zone in the Wülften-1 borehole ([34], **Figure 17**) would verify a correlation with explosive Siberian LIP-events. They would represent synchronous markers in contrast to the diachronounslithofacies/ichnofacies that migrated southward during Tethys transgression as an intermittent event between arid paleosol formation and the next flash flood (humid tropical climate).

The grey beds (tuff, ash?) generally relate to pelite and frequently to base resp. top of cycles (z 4 - 7, c 1 - 10) while the minor sandstone cycles in the Wülften-1 drill core appear asymmetrically within one cycle showing a steep ascent and a flat descent from base to top.

Table 3 exposes more or less striking concentrations of elements relevant in the exhalative phase of magmatism [51] [52] through the P-T transitional zone [17]. A few analytical data from the Um Irna F. are added (comp. **Table 2**). With regard to volatiles, *i.e.* As concentrations vary by 50 - 100 ppm in pelite of the Wulften-1 drill core, B varies between 506 - 1388 ppm in pelite and paleosol of the Um Irna F.

Furthermore, there is evidence for crustal assimilation by Ba, Rb, Th, K, Rb, Ta, Nb, Ce and Sn [54] while subalkaline rocks show a petrogenetic origin from a rather primitive mantle source and a plausible crustal overprint with intrusion temperatures of 915˚C - 1080˚C [52].

Primary crystals enclosed in ascending magma and originated in the deeper mantle, comprise droplets of the gas intrusions ("frozen Glass"). The latter show

Table 3. As, co minerals of the exhalative, hydrothermal and oxidation phase [51] [53].

Metal arsenides	Arsenic sulfides	Elemental arsenic	Arsenic oxide
Arsenopyrite (FeAsS)	Realgar (As_4S_4) Auripiment (As_2S_3)	Arsenic (As), (with strong acids → Arsenic acid)	Arsenolite (As_2O_3), → (weathering product)
Glanzcobalt (CoAsS)	Proustite (Ag_3AsS_3)		
Arsennickl (NiAsS)	Enargite (Cu_3AsS_4)		
Löllingite ($FeAs_2$)	Tennantite (Cu, Fe, Zn As_2S_3)		
Chloantite ($NiAs_{2-3}$)			
Rammelsbergite ($NiAs_{1-2}$)			
Safflorite ($CoAs_{2-3}$)			
Linnaeite Co_3S_4			

high levels of sulfur, chlorine and fluorine such as: 0.51 wt-% S, 0.94 wt-% Cl, 1.95 wt-% F [48] passing Paleozoic sedimentary source rocks, coal and hydrocarbons [45].

Degassing from the Siberian LIP is estimated on ~6300 - 7800 Gt S, ~3400 - 8700 GtCl and ~7100 - 13,600 Gt F, injected into the atmosphere and resulting in atmospheric hazard, acid rain ("lemon juice"), ocean acidification and more or less unknown chemical impact on continental surface rocks for an unique deterioration in global scale [48] [49].

The transfer of the eruptive gas/particle mixture took place from the magmatic source (including high amount of pre-eruptive origin from the magma chamber via troposphere (1/3 S) and stratosphere (1/2 S) to the depositional site [50].

Because of the lower located base of the atmosphere (7 - 10 km) in high latitude (as the Siberian LIP), the eruptive gas/particle column (up to 20 - 30 km) may faster reach the dry stratosphere [50]. Especially higher evolved magma may release eruptive column into the atmosphere to be carried away, within a few weeks, as a veil of some km in thickness. Thereby photochemical oxidation and reduction of SO_2 and H_2S react with H_2O to H_2SO_4 droplets (diameter < 1 mm) to remain up to ~3 a in the atmosphere prior to be settled on Earth [50].

As negative climate forcing, the effects of aerosol veils (H_2SO_4) and ash cause temperature decrease worldwide and ozone reduction (up to 70%) (**Figure 21**); H_2SO_4 reacts with NO_x to HNO_3 and with inactive Cl-reservoirs of the Stratosphere ($ClONO_2$, HCl) to reactive Cl and ClO that attacks the ozone layer (*i.e.* Pinatubo, 1991/92: 15% - 20% loss) [50].

Contrasting the negative climate forcing (−3.0 Wm^2), greenhouse gases (CO_2, CH_4, FCKW, NO_x) cause a temperature rise as positive climate forcing (+2.2 Wm^2 **Figure 21**). Thus, there occurredan interplay of both through the time-span of the Siberian LIP (at least from 252.33 to 251.3 Ma without possible

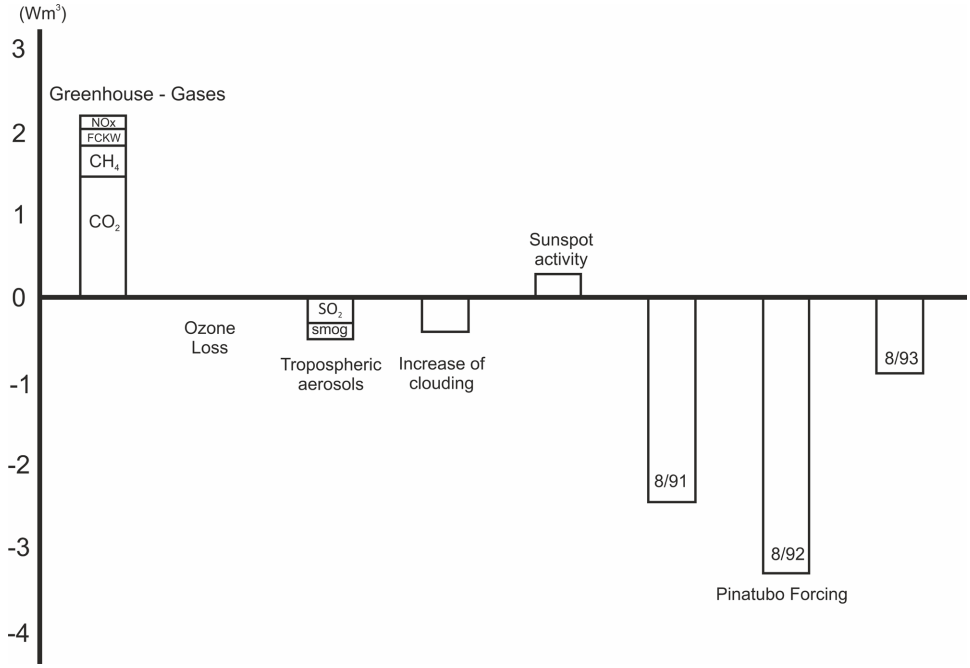

Figure 21. Interplay of positive and negative climate forcing [50]. Positive: by greenhouse gases (CO_2, CH_4, NO_x), sun radiation. Negative: by sulfate smog, tropospheric aerosols, clouding, tuff as [50].

precursor's tailings!) which mainly directs the P-T transitional zone via climate change.

5. Discussion and Conclusions: P-T Transitional Sedimentological/Mineralogical Patterns Meet Siberian LIP Degassing Effects

The main pulse (252.3 - 251.3 Ma) followed by recurrent magmatism (250.8 - 250.4 Ma) provides the framework for correlation relating to "indirect effects" of this LIP degassing via climate change. The total time-span covers the Zechstein F. Z7 (~2 Ma) and the Buntsandstein Calvörde F. (su C1-C7 (~0.7 Ma)) in the Germanic Basin [33] [34] as well as part of the Khuff-Cycles B, A (~2.5 Ma) on the Arabian Plate [14] [15]. Most of this period is characterized by normal magnetization [38].

In a broader sense the P-T transitional zone on the Arabian Plate is embedded between both MFSs P 40 (~254 Ma) and Tr10 (~250.5 Ma) covering in total more or less a SB time-span of ~3.5 Ma [14] [15].

The onset of mass extinction was determined on 251.9 Ma [26] [42] during magmatism in the Tunguska Basin. The foraminifera Cornuspiramabajeri encountered in the Nimra M. wackestone was interpreted as an opportunistic "disaster species" in a survival phase after mass extinction and prior tothe recovery phase [12] [22]. This subject is in detail discussed on a micropaleontologic basis [20]. So the focus of faunal recovery is directed to the MFS Tr 10 (250.5 Ma), [14] [15]. Thus, the following correlation attempts may be rich in meaning.

- The lower/upper M. unconformity of the Um Irna F. may coincide with the unconformity of the Lower/Upper Fulda F., Germanic Basin, however questionable because of missing radiometric age data (~251 Ma).
- A significant change of the mineral assemblage and Eh/pH conditions passing the Um Irna F./Himara M. transitional zone by changing sedimentary environment during transgression.
- Similar lithofacies cycles in the Um Irna F. and in the Fulda F. Germanic Basin (humid tropical FUC → arid DUP).
- Continuation of minor FUCs in the Lower Triassic Ma'in F. in the Buntsandstein Calvörde F. (Hessian Basin). The cycles of the latter F. can be precisely traced between Netherlands and Poland!
- Parts of the Khuff Cycles B, A, Arabian Plate relate to the P-T transitional zone in Jordan.
- The ?tuff/ash beds intercalated in the Siberian LIP suite, may partially correlate with the grey pelite beds in the Um Irna F. as well as in the drill core Wülften-1, Germanic Basin. The colored column of the latter does promise a higher number of tuff-layers (**Figure 17**).
- Toxic metals (As, Co, Cu, Zn, Pb) analyzed in Wülften-1 may be correlated to the exhalative phase of the Siberian LIP-Complex (**Figure 17** and **Figure 18**).
- Sequence-Analytical patterns (MFSs, SBs) and the Khuff Cycles B, A on the Arabian Platform may be correlated to the Substage Boundaries within the P-T transitional zone recovered via $\partial^{13}O$ excursions by astronomical tuning ([37] [40], **Figure 18**).
- Accepting the tuff-character of the thin grey pelite beds intercalated in the Um Irna F. sequence, Jordan between paleosol and overlying FUC (**Figure 10**), one may assume initial tuff eruption from the Siberians LIP, followed by magmatic intrusion/effusion that brought atmospheric hazard and climate change by degassing , after a long period (10^4 a) of arid climate in low latitudes, Arabian Plate, to initiate the interplay of greenhouse gas effect, aerosols, ozon layer reduction and toxic metal's impact onmarine (90%) and continental fauna extinction (70%) [40] [49].

As astronomical tuning throughout the P-T transitional zone exhibits, Milankovitch-Croll cycles may play an important role in the Feed Back System on the Earth [37] [54] [55] [56]. That concerns the following three perturbations:

- The change of Sun-Earth distance by the ellipticity of the Earth's orbit in 100.000 a cycles during which the solar input to the atmosphere may change by 30% of the current global average. This is shown in the case of the Lower Buntsandstein, Germanic Basin [33] [34].
- The obliquity of the Earth's axis (21.8˚ - 24.4˚) cause cycles of 40.000 a.
- The precession of the equinoxes affects the variation of the Sun-Earth distance causing solar irradiation (21.000 a cycles).

Both the latters are relevant for the time-span of drying upward paleosol formation throughout the Um Irna F., Jordan [17] [28].

Furthermore, the Moon becomes relevant as an acting force in the Earth's Feedback System [55] [56]: from 290 to 220 Ma its recession rate exhibits a slowdown from 110.31 km/Ma to 50.76 km/Ma according to Kepler's 3rd Planetary Law, accompanied by a sea level rise from −30 m (~250 Ma) to +75 m (~220 Ma) and a steep fall of the Earth's magnetic field that meets a maximum sea level rise (**Figure 22**), compare **Figure 18**.

Table 4 evidences a temporal coincidence of the Moon's recession rate and the spin angular velocity of the Earth with the Siberian LIP activity as well as with Upper Triassic impacting followed by the volcanism too [55] [56].

Compiling the most important processes in the Earth's feedback system applied to our subject [55].

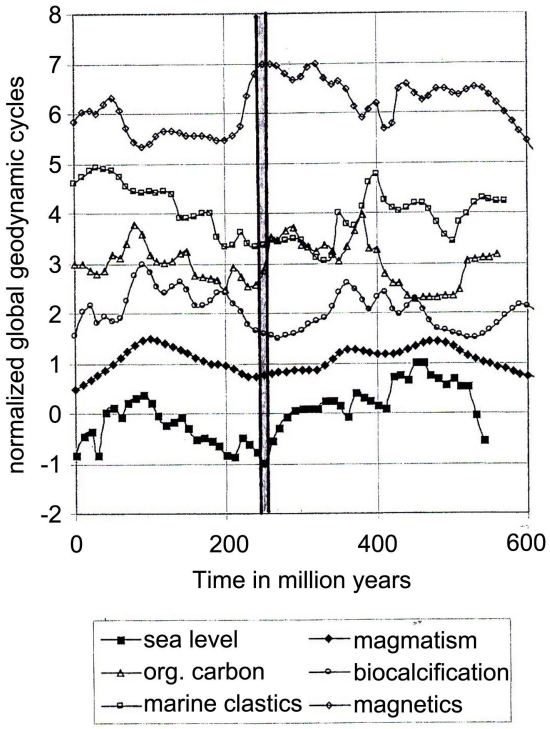

Figure 22. The P-T transitional zone, Jordan (253 - 249 Ma) projected into the interplay of a couple of Earth's Feedback System Players [55].

Table 4. Siberian LIP activity (252 - 250 Ma) and Upper Triassic impacting (219 - 214 Ma) followed by volcanism (202 - 201 Ma) temporarily relate to the Moon's recession rate (km/Ma) and the spin angular velocity of Earth (days/month) [55].

Ma	Moon's recession rate (km/Ma)		Spin angular velocity of the Earth (days/month)
153	18.66 volcanism impacting	↑	30.15 deceleration
220	59.76 Siberian LIP	↑	29.66 acceleration
290	110.31		30.16

- Earth's rotation slowing down and Moon recession cause variations of the Earth Mantle rotation and relating motion of the Earth's Core.
- Earth's magnetic field borne at the core/mantle boundary, provides in case of normal magnetization increased magmatic transport within convection cells in the mantle , developing plumes, high spreading rates of MORBs and relevant plate motion.

Consequences: Rising sea level, growing shelf areas, maximal magmatic emplacement up to ~10 Ma delaying after shelf development, long-lasting magmatic degassing.

Thus, rising sea level (TST), shelf development (tidal dissipation), normal magnetization during complete activity of the Siberian LIP (at least 2 Ma) are coupled with the opening of the Neo-Tethys, MORB activity, and the Siberian Plume event.

Further aspects of feedback systems with special regard to formation boundaries can be efficiently discussed by the creative compilations as by (*i.e.* [57] [58] [59] [60]).

Thus, it becomes evident: the more methods applied to the same subject the more we remove from "well-defined results" to "transitional zone data ("Unschärfe" sensu AUTOPOIESIS [61]). It seems that abiotic processes in the fields of Geosciences may underlay similar principles as of Biology, characterized as follows:

6. Closing Statement

"We do regard evolution as a structural drifting during continuous phylogenetic selection: there is no progress senso improvement of environmental use (exploitation) but merely the maintenance of adaption and autopoiesis (self-regulation) in a process where organism and environment remain in a lasting structural interplay".

H. E. Maturana and F. J. Varela, Biologists [61], transl. Sch.

Applied to Geoscience:

We, the authors, regard Earth History and accordingly Formation Boundaries as a structural drifting during a more or less continuous unstable equipoise. There is no restrained process concerning the improvement of the state of matter, but merely the maintenance of physical/chemical adaption and self-regulation (autopoiesis) under continuously changing conditions.

Parameters like P, T, pH, and Eh play a dominant role in the dissolution, transformation, and neoformation of minerals and sedimentary rocks during cosmic influence, climate forcing by LIP degassing, metamorphism, and diagenesis. Substitution, polymorphy, isomorphy, disorder, paragenesis, and replacement represent an entertaining interplay in the crystal lattice scale.

Acknowledgements

As the most important basics for the interpretation of the Siberian LIP effects on Sedimentary Geology/Mineralogy we especially appreciate the publications of B.

S. Amireh, D. E. Augland *et al.*, M. O. Clarkson *et al.*, M. Hiete *et al.*, and I. M. Makhlouf *et al.* We are grateful to Kjell Paris for digital support.

Conflicts of Interest

The authors declare no conflicts of interest regarding the publication of this paper.

References

[1] Walter Jens, W. (1987) Das A und das O. Die Offenbarung des Johannes. Radius Verlag, Stuttgart, 93 p.

[2] Tollmann, A. and Tollmann, E. (1993) Und die Sintflut gab es doch. Vom Mythos zur historischen Wahrheit, München, 560 p.

[3] Koch, H.P. (2000) The Diluvian Impact. P. Lange, Europ. Verlag der Wissensch, New York, Wien, 274 p.

[4] Schneider, W. and Salameh, E. (2012) Did Major Impacts Affect Sedimentologic/ Sequence-Analytical Patterns of the Early Palaeozoic Sedimentary Systems of Jordan, Arabian Plate? *Open Journal of Geology*, **2**, 241-252. https://doi.org/10.4236/ojg.2012.24024

[5] Schneider, W. and Salameh, E. (2020) Phanerozoic Quartz Arenite Formation and Sequence Analytical Patterns: Indirectly Relating to Major Impacting and Super Plume Volcanism, Jordan, Arabian Plate. *Open Journal of Geology*, **10**, 13-52. https://doi.org/10.4236/ojg.2020.101002

[6] Schneider, W. and Salameh, E. (2020) End-Cretaceous Quartz Arenite Formation in an Estuarian Environment under Brine Influence, N. Germany; Linked to both Deccan Volcanism and Chicxulub Impact Degassing during Climate Change. *Open Journal of Geology*, **10**, 1091-1118. https://doi.org/10.4236/ojg.2020.1011053

[7] Schneider, W. and Salameh, E. (2018) How to Trace out Impact-Triggered Effects Globally Scattered around Formation Boundaries: Case Uhry, North Germany (Eocene / Oligocene Boundary). *Open Journal of Geology*, **8**, 9-32. https://doi.org/10.4236/ojg.2018.81002

[8] Price, N.J. (2001) Major Impacts and Plate Tectonics. Routledge, London, 354 p. https://doi.org/10.1201/9780203165454

[9] Frisch, W. and Meschede, M. (2009) Plattentektonik. Kontinentverschiebung und Gebirgsbildung, 3. Auflage, Primus Verlag, Darmstadt, 196 p.

[10] Peterson, S.V., Dutton, A. and Lohman, K.C. (2016) End-Cretaceous Extinction in Antarctica Linked to Both Deccan Volcanism and Meteoritic Impact via Climate Change. *Nature Communications*, **7**, Article No. 12079. https://doi.org/10.1038/ncomms12079

[11] Henehan, M.J., Ridgwell, A., Thomas, E., Zhang, S., Alegret, L., Schmidt, J.R., Planavsky, N.J. and Hull, P.M. (2019) Rapid Ocean Acidification and Protracted Earth System Recovery Followed the End-Cretaceous Chicxulub Impact. *Proceedings of the National Academy of Sciences of the United States of America*, **116**, 22500-22504. https://doi.org/10.1073/pnas.1905989116

[12] Powell, J.H., Stephenson, M.H., Nicora, A., Rettori, R., Borlenghi, L.M. and Cristina Perri, M.C. (2016) The Permian-Triassic Boundary, Dead Sea, Jordan: Transitional Alluvial to Marine Depositional Sequences and Biostratigraphy. *Rivista Italiana di Paleontologia e Stratigrafia*, **122**, 23-40.

[13] Ziegler, M.A. (2001) Late Permian to Holocene Paleofacies Evolution of the Arabian Plate and its Hydrocarbon Occurrences. *GeoArabia*, **6**, 445-504. https://doi.org/10.2113/geoarabia0603445

[14] Sharland, P.R., Casey, D.M., Davies, R.B., Simmons, M.D. and Sut-Cliffe, O.E. (2004) Arabian Plate Sequence Stratigraphy—Revisions to SP2. *GeoArabia*, **9**, 199-214. https://doi.org/10.2113/geoarabia0901199

[15] Haq, B.U. and Al-Qahtani, A.M (2005) Phanerozoic Cycles of Sea-Level Change on the Arabian Platform. *GeoArabia*, **10**, 127-160. https://doi.org/10.2113/geoarabia1002127

[16] Bandel, K. and Khoury, H. (1981) Lithostratigraphy of the Triassic in Jordan. *Facies*, **4**, 1-26. https://doi.org/10.1007/BF02536584

[17] Makhlouf, I.M., Turner, B.R. and Abed, A.M. (1991) Depositional Facies and Environments in the Permian Umm Irna Formation, Dead Sea Area, Jordan. *Sedimentary Geology*, **73**, 117-139. https://doi.org/10.1016/0037-0738(91)90026-A

[18] Stephenson, M.H. and Powell, J.H. (2013) Palynology and Alluvial Architecture in the Permian Umm Irna Formation, Dead Sea, Jordan. *GeoArabia*, **18**, 17-60. https://doi.org/10.2113/geoarabia180317

[19] Stampfli, G.M. and Borel, G. (2002) A Plate Tectonic Model for the Palaeozoic and Mesozoic Constrained by Dynamic Plate Boundaries and Restored Synthetic Oceanic Iso-Chrones. *Earth and Planetary Science Letters*, **196**, 17-33. https://doi.org/10.1016/S0012-821X(01)00588-X

[20] Abu Hamad, A. (2004) Palaeobotany and Palynostratigraphy of the Permo-Triassic in Jordan. PhD Thesis, University of Hamburg, Hamburg, 330 p.

[21] Kerp, H., Abu Hamad, A., Vörding, B. and Bandel, K. (2006) Typical Triassic GondwanaFloral Elements in the Upper Permian of the Paleotropics. *Geology*, **34**, 265-268. https://doi.org/10.1130/G22187.1

[22] Stephenson, M.H. and Powell, J.H. (2014) Selected Spores and Pollen from the Permian Umm Irna Formation, Jordan, and their Stratigraphic Utility in the Middle East and North Africa. *Rivista Italiana di Paleontologia e Stratigrafia*, **120**, 145-156.

[23] Bandel, K. and Waksmundski, B. (1985) Triassic Conodonts from Jordan. *Acta Palaeontologica Polonica*, **35**, 289-304.

[24] Sadeddin, W. (1998) ConodontBiostratigraphy and Paleogeography of the Triassic in Jordan. *Palaeontographica Abteilung A*, **248**, 119-144. https://doi.org/10.1127/pala/248/1998/119

[25] Powell, J.H. and Molid, B.K. (1993) Structure and Sedimentation of Permo-Triassic Rocks Exposed in Small-Scale Horsts and Grabens of Pre-Cretaceous Age, Dead Sea Margin. *Journal of African Earth Sciences* (*and the Middle East*), **17**, 131-143. https://doi.org/10.1016/0899-5362(93)90031-K

[26] Augland, L.E., Ryabov, V.V., Vernikovsky, V.A., Planke, S., Polozov, A.G., Callegaro, S., *et al.* (2019) The Main Pulse of the Siberian Traps Expanded in Size and Composition. *Scientific Reports*, **9**, Article No. 18723. https://doi.org/10.1038/s41598-019-54023-2

[27] Miall, D. (1996) The Geology of Fluvial Deposits. Springer-Verlag, Berlin, Heidelberg, New York, 582 p.

[28] Amireh, B.S. (1987) Sedimentological and Petrological Interplays of the Nubian Series in Jordan with Regard to Paleogeography and Diagenesis. Doctoral Dissertation, Technische Universität Carolo Wilhelmina zu Braunschweig, Geology-Paleontology Dissertation, 7, 232 p., 33 Fig., 6 Tables, 16 Plates.

[29] Stow, D.A.V. (1986) Deep Clastic Seas. In: Reading, H.S., Ed., *Sedimentary Environments and Facies*, 2nd Edition, Blackwell Science Inc Publisher, Oxford, 399-444.

[30] Schneider, W., Abed, A. and Salameh, E. (1984) Mineral Content and Diagenetic Patterns—Useful Tools for Lithostratigraphic Subdivisions and Correlation of the Nubian Series: Results of Work in the Wadi Zerqa-Ma'in Area. *Schweizerbart'sche Verlagsbuchhandlung. Geol. Jb. B* 53, **B3**, 55-75.

[31] Uhl, D., Abu Hamad, A., Kerp, H. and Bandel, K. (2007) Evidence for Palaeo-Wildfire in the Permian Palaeotropics—CharcoalifiedWood from the Um Irna Formation of Jordan. *Review of Palaeobotany and Palynology*, **144**, 221-230. https://doi.org/10.1016/j.revpalbo.2006.08.003

[32] Ziegler, P.A. (1990) Geological Atlas of Western and Central Europe. Shell International Petroleum Maatsch. B. V., Hague, 239 p.

[33] Hug, N. and Gaupp, R. (2006) PalaeogeographicReconstruction in Red beds by Means of Genetically Related Correlation: Resultsfrom the Upper Zechstein (Late Permian). *Zeitschrift der Deutschen Gesellschaft für Geowissenschaften*, **157**, 107-120. https://doi.org/10.1127/1860-1804/2006/0157-0107

[34] Hiete, M., Berner, U., Heunisch, C. and Röhling, H.G. (2006) A High-resolution Inorganic Geochemical Profile across the Zechstein-BuntsandsteinBoundary in the North German Basin. *Zeitschrift der Deutschen Gesellschaft für Geowissenschaften*, **157**, 77-105. https://doi.org/10.1127/1860-1804/2006/0157-0077

[35] German Stratigraphic Commission (Ed.) (2002) Stratigraphic Table of Germany, Explanation. German Stratigraphic Commission, Potsdam, 16 p.

[36] Best, G. (1989) Die Grenze Zechstein/Buntsandstein in NW-Deutschland nach Bohrlochmessungen. *Zeitschrift der Deutschen Geologischen Gesellschaft*, **140**, 73-85. https://doi.org/10.1127/zdgg/140/1989/73

[37] Li, M., Ogg, J., Zhang, Y., Huang, C., Hinnov, L., Chen, Z.-Q. and Zou Z. (2016) Astronomical Tuning of the End-Permian Extinction and the Early Triassic Epoch of South China and Germany. *Earth and Planetary Science Letters*, **441**, 10-25. https://doi.org/10.1016/j.epsl.2016.02.017

[38] Burgess, N. and Skurlies, M. (2006) Kontenentale Perm-TriasGrenze und BuntsandsteinNördlich von Halle (Saale). Fazies, Biologie, Zyklen und Magnetostratigraphie (Exkursion M am 22. April 2006). *Jahresberichte und Mitteilungen des Oberrheinischen Geologischen Vereins*, **88**, 427-452. https://doi.org/10.1127/jmogv/88/2006/427

[39] Burgess, S.D., Bowring, S. and Shen, S.Z. (2014) High-precision Timeline for Earth's Most Severe Extinction. *Proceedings of the National Academy of Sciences of the United States of America*, **111**, Article ID: 201317692. https://doi.org/10.1073/pnas.1317692111

[40] Clarkson, M.O., Richozb, S., Wood, R.A., Maurer, F.W., Krystyn, L., McGurty, D.J. and Astratti, D. (2013) A New High-Resolution $\delta^{13}C$ Record for the Early Triassic: Insights from the Arabian Platform. *Gondwana Research*, **24**, 233-242. https://doi.org/10.1016/j.gr.2012.10.002

[41] Reichow, M.K., Malcolm, P., Al'Mukhamedov, A.J., Allen, M.B., Andreichev, V.L., Buslov, M.M., *et al.* (2009) The Timing and Extent of the Eruption of the Siberian Traps Large Igneous Province: Implications for the End-Permian Environmental Crisis. *Earth and Planetary Science Letters*, **277**, 9-20. https://doi.org/10.1016/j.epsl.2008.09.030

[42] Burgess, S.D. and Bowring, S.A. (2015) High-precision Geochronology Confirms

Voluminous Magmatismbefore, during, and after Earth's Most Severe Extinction. *Science Advances*, **1**, e1500470. https://doi.org/10.1126/sciadv.1500470

[43] Galfetti, T., Bucher, H., Ovtcharova, M., Schaltegger, U., Brayard, A., Brühwiler, T., *et al.* (2007) Timing of the Early Triassic Carbon Cycle Perturbations Inferred from New U-Pb Ages and Ammonoid Biochronozones. *Earth and Planetary Science Letters*, **258**, 593-604. https://doi.org/10.1016/j.epsl.2007.04.023

[44] Ovtcharova, M., Bucher, H., Schaltegger, U., Galfetti, T., Brayard, A. and Guexet, J. (2006) New Early to Middle Triassic U-Pb Ages from South China: Calibration with AmmonoidBiochronozones and Implications for the Timing of the Triassic Biotic Recovery. *Earth and Planetary Science Letters*, **243**, 463-475. https://doi.org/10.1016/j.epsl.2006.01.042

[45] Svensen, H., Planke, S., Polozov, A.G., Schmidbauer, N., Corfu, F., Podladchikov, Y.Y., *et al.* (2009) Siberian Gas Venting and the End-Permian Environmental Crisis. *Earth and Planetary Science Letters*, **277**, 490-500. https://doi.org/10.1016/j.epsl.2008.11.015

[46] Gold, Th. (2001) Biosphaere der HeissenTiefe. 2 Aufl., Ed. Steinherz, Wiesbaden, 256 p.

[47] Walderhaug, H. J., Eide, E. A., Scott, R. A., Inger, S. and Golionko, E. G. (2005) Palaeomagnetism and $^{40}Ar/^{39}Ar$ Geochronology from the South Taimyr Igneous Complex, Arctic Russia: a Middle-Late Triassic Magmatic Pulse after Siberian Flood-Basalt Volcanism. *Geophysical Journal International*, **163**, 501-517. https://doi.org/10.1111/j.1365-246X.2005.02741.x

[48] Black, B.A., Elkins-Tanton, L.T., Rowe, M.C. and Peate, I.U. (2012) Magnitude and Consequences of Volatile Release from the Siberian Traps. *Earth and Planetary Science Letters*, **317-318**, 363-373. https://doi.org/10.1016/j.epsl.2011.12.001

[49] Elkins-Tanton, L.T. (2015) Siberian Flood Basalts: The Earth's Largest Extinction and Climate Change. *Future Tense*, 31.

[50] Schmincke, H.U. (2000) Vulkanismus. Wissenschaftliche Buchgesellschaft Darmstadt, 264 p.

[51] Correns, C.W. (1968) Einführung in die Mineralogie. 2 Aufl., Springer, Berlin, 458 p. https://doi.org/10.1007/978-3-662-25929-0

[52] Krauskopf, K.B. (1982) Introduction to Geochemistry. McGraw-Hill International, London, 617 p.

[53] Hollemann, A.F. (1964) Lehrbuch der Anorganischen Chemie. DeGruyter & Co., Berlin, 766 p. https://doi.org/10.1515/9783112312889

[54] Hughes, P.N.J. and Mason, N.J. (2001) Introduction to Environmental Physics Planet Earth, Life and Climate. CRC Press, London, New York, 463 p. https://doi.org/10.1201/9781482273069

[55] Brink, H.-J. (2006) Do the Global Geodynamic Cycles of the PharenozoicRepresent a Feedback System of the Earth and is the Moon Involved as an Acting External Force? *Zeitschrift der Deutschen Gesellschaft für Geowissenschaften*, **157**, 17-40. https://doi.org/10.1127/1860-1804/2006/0157-0017

[56] Creer, K.M. (1975) On the Tentative Correlation between Changes in the Geomagnetic Polarity Bias and Reversals Frequency and the Earth's Rotation through Phanerozoic Time. In: Rosenberg, G.D. and Runcorn, S.K., Eds., *Growth Rhythms and the History of the Earth's Rotation*, Wiley, London, 293-318.

[57] Self, S., Schmidt, A. and Mather, T.A. (2014) Emplacement Characteristics, Time Scales, and Volcanic Gas Release Rates of Continental Flood Basalt Eruptions on

Earth. In: Keller, G. and Kerr, A.C., Eds., *Volcanism, Impacts, and Mass Extinctions: Causes and Effects*, Vol. 505, Geological Society of America, Boulder, 319-337. https://doi.org/10.1130/2014.2505(16)

[58] Svensen, H.H., Jerram, D.A., Polozov, A.G., Planke, S., Neal, C.R., Augland, L.E., *et al.* (2019) Thinking about LIPs: A Brief History of Ideas in Large Igneous Province Research. *Tectonophysics*, **760**, 229-251. https://doi.org/10.1016/j.tecto.2018.12.008

[59] Svensen, H.H., Torsvik, T.H., Callegaro, S., Augland, L., Heimdal, T.H., Jerram, D.A., *et al.* (2018) Gondwana Large Igneous Provinces: Plate Reconstructions, Volcanic Basins and Sill Volumes. In: Sensarma, S. and Storey, B.C., Eds., *Large Igneous Provinces from Gondwana and Adjacent Regions*, Vol. 463, Geological Society of London, London, 17-40. https://doi.org/10.1144/SP463.7

[60] Abdelmalak, M.M., Planke, S., Polteau, S., Hartz, E.H., Faleide, J.I., Tegner, C., *et al.* (2018) Break-Up Volcanism and Plate Tectonicscin the NW Atlantic. *Tectonophysics*, **760**, 267-296. https://doi.org/10.1016/j.tecto.2018.08.002

[61] Maturana, H.R. and Varela, F.J. (1984) Der Raum der Erkenntnis. Die Biologischen Wurzeln des Menschlichen Erkenntnis. Goldmann G. 1490/11460, Scherz Verlag, München, 280 p.